Research Square

Preprints are preliminary reports that have not undergone peer review.
They should not be considered conclusive, used to inform clinical practice,
or referenced by the media as validated information.

Dynamics of a fractional reaction–diffusion epidemic model

Md Shah Alam

malam@htu.edu

Huston–Tillotson University https://orcid.org/0009-0004-3765-4953

Research Article

Keywords: Fractional diffusion, Nonlocal epidemic model, Nonlocal asymptomatic transmission, Intermittent treatment, Global existence and asymptotic behavior

Posted Date: August 14th, 2026

DOI: https://doi.org/10.21203/rs.3.rs-10672645/v1

License: This work is licensed under a Creative Commons Attribution 4.0 International License.
Read Full License

Additional Declarations: The authors declare no competing interests.

Dynamics of a fractional reaction–diffusion epidemic model

Md Shah Alam*

Department of Mathematics, Huston-Tillotson University, Austin, TX 78702, USA

Abstract

We investigate the global dynamics of a spatiotemporal epidemic model with regional fractional diffusion, nonlocal asymptomatic transmission, crowding-dependent disease incidence, and periodic intermittent treatment. The proposed model captures the combined effects of long-range dispersal, hidden infection pathways, population crowding, and time-dependent intervention strategies. By combining semigroup theory with robust L^p estimates, we establish the global existence, uniqueness, positivity, uniform boundedness, and asymptotic behavior of classical solutions. To complement the theoretical analysis and provide further insight into the model dynamics, numerical simulations are performed to illustrate the effects of the fractional diffusion order, nonlocal asymptomatic transmission, intermittent treatment, and population crowding.

AMS Subject Classification [2020]: 35R11, 35K57, 92D30, 35R09, 47G20, 35K91

Keywords: Fractional diffusion; Nonlocal epidemic model; Nonlocal asymptomatic transmission; Intermittent treatment; Global existence and asymptotic behavior.

1 Introduction and Main Results

1.1 Introduction

Spatiotemporal epidemic models provide a fundamental framework for understanding the spread of infectious diseases in heterogeneous environments and for designing effective intervention strategies. By integrating disease transmission with spatial dispersal, these models offer a more realistic description of epidemic dynamics than purely temporal formulations. Consequently, they have been extensively employed to investigate disease persistence, spatial propagation, traveling waves, pattern formation, optimal control, and numerical simulations; see, for example, [4,35,37,39,41,42,45,51,52] and the references therein.

A broad class of spatiotemporal epidemic models is formulated as reaction–diffusion systems (RDS), where diffusion terms describe the spatial movement of individuals and reaction terms characterize local disease transmission and progression. Although classical reaction–diffusion models have proved highly successful in describing spatial epidemic dynamics, the underlying local diffusion assumption may be inadequate for representing long-range human mobility associated with migration, commuting, and modern transportation networks.

The increasing connectivity of modern societies through urbanization, international travel, and transportation networks has substantially enhanced long-range interactions among populations, allowing disease transmission to occur between geographically distant regions through the movement of infected individuals or indirect contacts. Nonlocal diffusion naturally accounts for such long-range dispersal, while nonlocal reaction terms describe disease transmission arising from interactions between individuals located at different spatial positions. Consequently, nonlocal epidemic models provide a more realistic framework for studying disease spread in heterogeneous environments and have attracted considerable attention in

*Email: malam@htu.edu

recent years. Extensive studies have been devoted to their analytical, qualitative, and numerical properties [5, 11, 12, 14, 17–19, 28, 31, 32, 49, 50, 53–55, 57, 58].

Among nonlocal dispersal mechanisms, fractional diffusion operators have emerged as an effective framework for modeling anomalous diffusion and Lévy-type long-range movement beyond the classical Brownian paradigm. Their ability to capture nonlocal interactions over multiple spatial scales makes them particularly suitable for epidemic models involving long-range dispersal. Consequently, fractional epidemic models have received considerable attention, and their well-posedness, persistence, spreading dynamics, traveling waves, and optimal control have been well studied in [6, 7, 10, 16, 26, 27, 47]. In particular, the regional fractional Laplacian provides a natural framework for describing long-range dispersal within bounded habitats, making it especially suitable for spatial epidemic models defined on finite geographical domains [3].

Asymptomatic transmission is a defining feature of many infectious diseases, including COVID–19, influenza, and dengue fever. Because asymptomatic individuals are less likely to be detected or isolated, they often continue their routine activities and may spread infection over broad spatial scales through human mobility and social interactions. This naturally motivates the use of a nonlocal incidence mechanism to describe infections generated by asymptomatic individuals, thereby accounting for disease transmission beyond local neighborhoods. In addition, the intensity of disease transmission is strongly influenced by population crowding, since densely populated environments such as transportation hubs, schools, refugee camps, hospitals, and urban areas substantially increase contact opportunities and facilitate disease spread. Incorporating a crowding-dependent transmission factor into the nonlocal incidence therefore provides a more realistic description of epidemic dynamics by capturing the combined effects of long-range human mobility and local population density. Related studies on asymptomatic transmission, nonlocal force of infection, crowd influence, and their relation with spatial epidemic dynamics can be found in [2, 9, 21, 22, 24, 25, 33, 34, 38, 46, 56, 59] and the references therein.

Periodic treatment strategies are widely used in infectious disease control. Owing to limited healthcare resources, economic constraints, and scheduled public health programs, treatment is often implemented intermittently rather than continuously. Such intervention protocols have been investigated in epidemic models; see, for example, [23, 29, 44].

Motivated by the above observations, we propose a spatiotemporal epidemic model that integrates regional fractional diffusion, a nonlocal incidence mechanism for asymptomatic transmission, crowding-dependent disease transmission, and periodic intermittent treatment within a unified framework. The proposed model captures key features of real-world epidemics, including long-range human mobility, hidden transmission through asymptomatic individuals, population-density effects, and time-dependent intervention strategies. To the best of our knowledge, this is the first rigorous analytical study of a fractional epidemic model that simultaneously incorporates these mechanisms. The interaction of fractional diffusion, nonlocal transmission, and intermittent treatment introduces significant analytical challenges, while providing new insights into disease dynamics and control.

Let $n \in \mathbb{N}$ and let $\Omega \subset \mathbb{R}^n$ be a bounded open subset with smooth boundary $\partial\Omega$, where $\partial\Omega$ is an $(n-1)$-dimensional $C^{2+\varrho}$-manifold for some $\varrho \in (0,1)$, and Ω lies locally on one side of $\partial\Omega$.

We consider the following epidemic model:

$$
\begin{cases}
S_t(x,t) = d_S(-\Delta)^{\alpha} S(x,t) + b(x) - S(x,t)g(x,t) - \mu(x)S(x,t), & (x,t) \in \Omega \times (0,\infty),\\
I_{1_t}(x,t) = d_{I_1}(-\Delta)^{\alpha} I_1(x,t) + \sigma(x)S(x,t)g(x,t) - \Big(\lambda_1(x) + \mu(x)\Big)I_1(x,t), & (x,t) \in \Omega \times (0,\infty),\\
I_{2_t}(x,t) = d_{I_2}(-\Delta)^{\alpha} I_2(x,t) + \Big(1-\sigma(x)\Big)S(x,t)g(x,t) - \Big(\lambda_2(x) + \mu(x) + \delta(x) + \gamma(x,t)\Big)I_2(x,t),\\
\qquad\qquad (x,t) \in \Omega \times (0,\infty),\\
R_t(x,t) = d_R(-\Delta)^{\alpha} R(x,t) + \lambda_1(x)I_1(x,t) + \Big(\lambda_2(x) + \gamma(x,t)\Big)I_2(x,t) - \mu(x)R(x,t), & (x,t) \in \Omega \times (0,\infty),\\
\mathcal{N}_{\alpha} S = \mathcal{N}_{\alpha} I_1 = \mathcal{N}_{\alpha} I_2 = \mathcal{N}_{\alpha} R = 0, & (x,t) \in (\mathbb{R}^n \setminus \Omega) \times (0,\infty),\\
\Big(S(x,0), I_1(x,0), I_2(x,0), R(x,0)\Big) = \Big(S_0(x), I_{1,0}(x), I_{2,0}(x), R_0(x)\Big) \geq 0, & x \in \Omega,
\end{cases}
\tag{1.1}
$$

The functions $S(x,t)$, $I_1(x,t)$, $I_2(x,t)$, and $R(x,t)$ denote the densities of susceptible, asymptomatic infected, symptomatic infected, and recovered individuals, respectively, at location $x \in \Omega$ and time $t > 0$. Initial data

are assumed to be nonnegative and bounded. The force of infection is given by

$$g(x,t) = \int_\Omega \rho(x,y)\omega(y)\beta_1(y)I_1(y,t)\,dy + \beta_2(x)I_2(x,t), \quad \omega(y) = 1 + \kappa C(y).$$

The first term represents the nonlocal asymptomatic incidence and the second term accounts for the local transmission generated by symptomatic infected individuals. The functions $\rho(x,y)$, $\omega(y)$, and the remaining model parameters are described in Table 2.

For each compartment $u \in \{S, I_1, I_2, R\}$, the homogeneous nonlocal Neumann boundary condition is given by

$$\mathcal{N}_\alpha u(x,t) = C_{n,\alpha} \int_\Omega \frac{u(y,t) - u(x,t)}{|x-y|^{n+2\alpha}}\,dy = 0, \qquad (x,t) \in (\mathbb{R}^n \setminus \Omega) \times (0,\infty), \tag{1.2}$$

where $C_{n,\alpha} = \frac{4^\alpha \Gamma\left(\frac{n}{2}+\alpha\right)}{\pi^{n/2}|\Gamma(-\alpha)|}$ is the normalization constant and $\Gamma(z) = \int_0^\infty t^{z-1}e^{-t}\,dt$, $\mathrm{Re}(z) > 0$, denotes the Gamma function.

The condition (1.2) prevents individuals from entering or leaving the habitat through nonlocal dispersal and ensures that all spatial interactions remain confined to the domain Ω.

Consequently, the diffusion process is governed by the regional fractional Laplacian. For each $u \in \{S, I_1, I_2, R\}$, the operator admits the Riesz integral representation

$$(-\Delta)^\alpha u(x,t) = C_{n,\alpha}\,\mathrm{P.V.} \int_\Omega \frac{u(y,t) - u(x,t)}{|x-y|^{n+2\alpha}}\,dy, \quad (x,t) \in \Omega \times (0,\infty). \tag{1.3}$$

Biologically, the regional fractional Laplacian describes the nonlocal movement of individuals within the spatial domain. Unlike classical diffusion, which represents only local random movement, it permits occasional long-distance dispersal, with the likelihood of movement decreasing as the distance between locations increases. The fractional exponent $\alpha \in (0,1)$ governs the degree of nonlocality: smaller values of α correspond to heavier-tailed movement patterns and hence more frequent long-range travel.

The epidemiological parameters used in system (1.1) are summarized in Table 2.

Table 1: Description of the epidemiological parameters in system (1.1).

Parameter	**Description**
$\alpha \in (0,1)$	Order of the fractional diffusion operator.
$d_S > 0$	Diffusion coefficient of susceptible individuals.
$d_{I_1} > 0$	Diffusion coefficient of asymptomatic infected individuals.
$d_{I_2} > 0$	Diffusion coefficient of symptomatic infected individuals.
$d_R > 0$	Diffusion coefficient of recovered individuals.
$b(x) \geq 0$	Spatially heterogeneous recruitment rate of susceptible individuals.
$\beta_1(x) \geq 0$	Transmission rate associated with asymptomatic infected individuals.
$\beta_2(x) \geq 0$	Transmission rate associated with symptomatic infected individuals.
$\sigma(x) \in [0,1]$	Proportion of newly infected individuals who become asymptomatic.
$1 - \sigma(x)$	Proportion of newly infected individuals who become symptomatic.
$\mu(x) \geq 0$	Natural mortality rate.
$\lambda_1(x) \geq 0$	Recovery rate of asymptomatic infected individuals.
$\lambda_2(x) \geq 0$	Recovery rate of symptomatic infected individuals.

Continued on next page

Table 1 – Continued from previous page

Parameter	Description
$\delta(x) \geq 0$	Disease-induced mortality rate of symptomatic infected individuals.
$\gamma(x,t) \geq 0$	Spatially heterogeneous periodic treatment rate acting on symptomatic infected individuals.
$\rho(x,y) \geq 0$	Nonlocal transmission kernel describing the influence of infected individuals at location y on susceptibles at location x.
$\omega(y) \geq 1$	Crowding-dependent transmission factor.
$C(y) \geq 0$	Crowding intensity at location y.
$\kappa \geq 0$	Strength of crowding-induced transmission.

$\gamma(x,t) \geq 0$ represents a spatially heterogeneous treatment rate and is assumed to be bounded and periodic in time with period $T > 0$. For any $L \in (0,T)$, there exists a nonnegative function $\gamma_1(x,t)$, positive on a subset $\widehat{\Omega} \subset \Omega$ of positive measure. Moreover, there exist a constant $\gamma_0 > 0$ such that $\gamma_1(x,t) \geq \gamma_0,\ (x,t) \in \widehat{\Omega} \times [0,\infty)$, and

$$\gamma(x,t) = \begin{cases} 0, & x \in \Omega, \quad kT \leq t < (k+1)T - L, \quad k \in \mathbb{N} \cup \{0\}, \\ \gamma_1(x,t), & x \in \Omega, \quad (k+1)T - L \leq t < (k+1)T, \quad k \in \mathbb{N} \cup \{0\}. \end{cases}$$

Throughout each treatment cycle of duration T, therapeutic intervention is implemented only during the final L-time units. Consequently, no treatment is administered over the interval $kT \leq t < (k+1)T - L$, whereas symptomatic individuals receive treatment at rate $\gamma_1(x,t)$ during $(k+1)T - L \leq t < (k+1)T$. This periodic treatment protocol reflects intermittent intervention strategies commonly adopted in practice due to limited healthcare resources, seasonal treatment campaigns, or scheduled public health control programs.

We adopt the following notation throughout the paper where all the spatial parameters are continuous and bounded on $\overline{\Omega}$:

$$\begin{aligned}
&b^* := \max_{x\in\overline{\Omega}} b(x) \geq 0, \qquad \sigma^* := \max_{x\in\overline{\Omega}} \sigma(x) \in [0,1], \qquad \mu^* := \max_{x\in\overline{\Omega}} \mu(x) \geq 0, \qquad \mu_0 := \min_{x\in\overline{\Omega}} \mu(x) > 0, \\
&\delta^* := \max_{x\in\overline{\Omega}} \delta(x) \geq 0, \qquad \delta_0 := \min_{x\in\overline{\Omega}} \delta(x) > 0, \qquad \lambda_i^* := \max_{x\in\overline{\Omega}} \lambda_i(x) \geq 0, \qquad \lambda_{i,0} := \min_{x\in\overline{\Omega}} \lambda_i(x) > 0, \\
&\beta_i^* := \max_{x\in\overline{\Omega}} \beta_i(x) \geq 0, \qquad C^* := \max_{x\in\overline{\Omega}} C(x) \geq 0, \qquad \omega^* := \max_{x\in\overline{\Omega}} \omega(x) = 1 + \kappa C^*, \\
&\gamma^* := \max_{(x,t)\in\overline{\Omega}\times[0,T]} \gamma(x,t) \geq 0,
\end{aligned}$$

for $i = 1, 2$. For convenience, we write the reaction terms in system (1.1) as

$$\begin{cases}
f_1(x,t,S,I_1,I_2,R) &= b(x) - g(x,t)S(x,t) - \mu(x)S(x,t), \\
f_2(x,t,S,I_1,I_2,R) &= \sigma(x)g(x,t)S(x,t) - \Big(\lambda_1(x) + \mu(x)\Big)I_1(x,t), \\
f_3(x,t,S,I_1,I_2,R) &= \Big(1 - \sigma(x)\Big)g(x,t)S(x,t) - \Big(\lambda_2(x) + \mu(x) + \delta(x) + \gamma(x,t)\Big)I_2(x,t), \\
f_4(x,t,S,I_1,I_2,R) &= \lambda_1(x)I_1(x,t) + \Big(\lambda_2(x) + \gamma(x,t)\Big)I_2(x,t) - \mu(x)R(x,t).
\end{cases} \tag{1.4}$$

From a mathematical perspective, system (1.1) presents several analytical challenges arising from the regional fractional diffusion operator, the nonlocal incidence mechanism, the strong nonlinear coupling among the epidemiological compartments, and the spatial heterogeneity of the model coefficients. These features considerably complicate the derivation of global L^p estimates, the establishment of uniform boundedness, and the analysis of the long-time behavior of solutions.

To address these challenges, we establish the global existence, uniqueness, positivity, uniform boundedness, and asymptotic behavior of classical solutions by combining semigroup theory with robust L^p estimates.

In addition to the analytical results, we perform a series of numerical simulations to complement the theoretical analysis and provide a visual illustration of the model dynamics. These computations are not intended as independent mathematical evidence; rather, they serve to demonstrate the qualitative behavior predicted by the theory.

1.2 Statement of the Main Results

We assume that

(D) (Diffusivity) $d_S, d_{I_1}, d_{I_2}, d_R > 0$, $\rho \in C(\overline{\Omega} \times \overline{\Omega}, \mathbb{R}_+)$ such that $\rho(x, y) = \rho(y, x)$ for all $x, y \in \Omega$ and there exists a $\Lambda > 0$ such that

$$\int_\Omega \rho(x, y)\, dy \le \Lambda < \infty.$$

(Qp) (Quasi-positivity) The reaction vector field F is quasi-positive; that is, for every $(x, t) \in \overline{\Omega} \times [0, \infty)$ and every $(S, I_1, I_2, R) \in \mathbb{R}^4_+$, we have $f_1(x, t, 0, I_1, I_2, R) \ge 0$, $f_2(x, t, S, 0, I_2, R) \ge 0$, $f_3(x, t, S, I_1, 0, R) \ge 0$, $f_4(x, t, S, I_1, I_2, 0) \ge 0$.

Under (D), together with the boundedness assumptions on $\beta_i(x)$, $i = 1, 2$, and $\omega(x)$, the nonlocal force of infection $g(x, t)$ defines a bounded linear operator with respect to (I_1, I_2). Consequently, the incidence term is locally Lipschitz on bounded subsets of the positive cone. Hence, the reaction vector field is locally Lipschitz with respect to the state variables.

Additionally, biologically, $\rho(x, y)$ represents the transmission intensity from infected individuals located at y to susceptible individuals at x. The continuity of ρ ensures that transmission varies smoothly across the spatial domain, the symmetry assumes isotropic spatial interactions, and the uniform bound guarantees that the total infection pressure experienced at each location remains finite.

Theorem 1 *Assume that (D), (Qp) hold and $(S_0, I_{1,0}, I_{2,0}, R_0) \in L^\infty(\Omega; \mathbb{R}^4_+)$.Then there exists a unique classical global component-wise nonnegative solution $(S(x, t), I_1(x, t), I_2(x, t), R(x, t))$ to the system* (1.1)*. Moreover, each component remains uniformly bounded in the sup norm for all time.*

Theorem 2 *Assume that the hypotheses of Theorem 1, Lemma 2.3, and Lemma 2.4 hold. Let S^* denote the disease-free steady state satisfying* (2.15)*. If $S_0(x) \le S^*(x)$ for all $x \in \Omega$, then the unique classical global solution of system* (1.1) *satisfies*

$$\lim_{t\to\infty} \|I_1(\cdot, t)\|_{L^\infty(\Omega)} = \lim_{t\to\infty} \|I_2(\cdot, t)\|_{L^\infty(\Omega)} = \lim_{t\to\infty} \|S(\cdot, t) - S^*\|_{L^\infty(\Omega)} = 0.$$

The remainder of this paper is organized as follows. In Section 2, we establish the global well-posedness and asymptotic behavior of solutions to system (1.1). Numerical simulations are presented in Section 3. Finally, concluding remarks are given in Section 4.

2 Proof of Main Theorems

Since the equation for R is linear with forcing terms depending only on I_1 and I_2, it suffices to analyze the subsystem consisting of S, I_1, and I_2. The component R is then uniquely determined by the corresponding linear nonhomogeneous nonlocal equation.

We will use the following semigroup theory [43] to prove Theorem 1. Let us define, $X := L^2(\Omega)$, $X_+ := \{z \in X : z \ge 0 \text{ a.e. on } \Omega\}$. Define the operators $A_i z = d_i(-\Delta)^\alpha z$, $i \in \left\{S, I_1, I_2\right\}$ with domain

$$\mathcal{D}(A_i) = \left\{z \in H^\alpha(\Omega) : A_i z \in L^2(\Omega),\ \mathcal{N}_\alpha z = 0 \text{ on } \mathbb{R}^n \setminus \Omega\right\}.$$

The regional fractional Laplacian is associated with the bilinear form

$$\mathcal{E}_\alpha(u, v) = \frac{C_{n,\alpha}}{2} \int_\Omega \int_\Omega \frac{\Big(u(y) - u(x)\Big)\Big(v(y) - v(x)\Big)}{|x - y|^{n+2\alpha}}\, dx\, dy, \qquad u, v \in H^\alpha(\Omega).$$

where the corresponding fractional Sobolev space is defined by

$$H^{\alpha}(\Omega) := \left\{ u \in L^2(\Omega) : \int_{\Omega}\int_{\Omega} \frac{|u(y)-u(x)|^2}{|x-y|^{n+2\alpha}}\, dx\, dy < \infty \right\}.$$

The norm on $H^{\alpha}(\Omega)$ is given by

$$\|u\|^2_{H^{\alpha}(\Omega)} := \|u\|^2_{L^2(\Omega)} + \int_{\Omega}\int_{\Omega} \frac{|u(y)-u(x)|^2}{|x-y|^{n+2\alpha}}\, dx\, dy = \|u\|^2_{L^2(\Omega)} + [u]^2_{H^{\alpha}(\Omega)},$$

$$\text{where, } [u]^2_{H^{\alpha}(\Omega)} := \int_{\Omega}\int_{\Omega} \frac{|u(y)-u(x)|^2}{|x-y|^{n+2\alpha}}\, dx\, dy$$

denotes the Gagliardo seminorm [40, 48].

For each $i \in \{S, I_1, I_2\}$, the operator

$$A_i := d_i(-\Delta)^{\alpha}.$$

The operator A_i is a nonnegative self-adjoint operator on $L^2(\Omega)$ associated with the bilinear form $\mathcal{E}_{\alpha}$. Moreover, A_i generates a species-dependent strongly continuous analytic semigroup $\{T_i(t)\}_{t\geq 0}$ on $L^2(\Omega)$. In the absence of reaction terms, the corresponding diffusion process conserves the total population mass. For further details on the regional fractional Laplacian, the associated nonlocal Neumann boundary conditions, and their analytical properties, we refer the reader to [13, 15].

Introducing the product space $\mathbb{X} = L^2(\Omega) \times L^2(\Omega) \times L^2(\Omega)$, the diffusion part of system (1.1) can be represented by the block-diagonal operator

$$\mathcal{A} = diag(A_S, A_{I_1}, A_{I_2}) \text{ with } \mathcal{D}(\mathcal{A}) = \mathcal{D}(A_S) \times \mathcal{D}(A_{I_1}) \times \mathcal{D}(A_{I_2}).$$

Since each diagonal operator generates an analytic semigroup on $L^2(\Omega)$, it follows from standard product semigroup theory that $\mathcal{A}$ generates an analytic C_0-semigroup on $\mathbb{X}$,see, for instance, [8, 43]. Consequently, system (1.1) may be formulated as a semilinear evolution equation on $\mathbb{X}$, where the coupling is introduced solely through the reaction terms.

Next, we state and prove two auxiliary lemmas that play an important role in the proofs of Theorems 1 and 2.

Lemma 2.1 *Let S, I_1, I_2 be the unique nonnegative maximal solutions of the system (1.1) on the interval $[0, T_m)$ with $T_m \in (0, \infty]$. Then there exists an $M > 0$ such that $\int_{\Omega}\left(S + I_1 + I_2\right) dx \leq M$ for any $\mu_0 > 0$.*

Proof of Lemma 2.1: Let $u = (u_1, u_2, u_3) \equiv (S, I_1, I_2)$. Adding the first three equations of the system (1.1) and then integrating over Ω we get,

$$\begin{aligned}\int_{\Omega}\sum_{i=1}^{3} u_{i_t}(x,t)\, dx &\leq \int_{\Omega}\sum_{i=1}^{3} d_i(-\Delta)^{\alpha}u_i(x,t)\, dx + \int_{\Omega} b(x)\, dx - \int_{\Omega}\mu(x)\sum_{i=1}^{3} u_i(x,t)\, dx \\ &\leq b^* \int_{\Omega} dx - \mu_0 \int_{\Omega}\sum_{i=1}^{3} u_i(x,t)\, dx\end{aligned}$$

here we used $\int_{\Omega}\sum_{i=1}^{3} d_i(-\Delta)^{\alpha}u_i(x,t)\, dx = -\int_{\mathbb{R}^n\setminus\Omega}\sum_{i=1}^{3}\mathcal{N}_{\alpha}u_i(x,t)\, dx = 0$. Using the Grönwall's inequality to the above differential inequality we get,

$$\int_{\Omega}\Big(S(x,t) + I_1(x,t) + I_2(x,t)\Big)\, dx \leq M,\ t \in [0, T_m)$$

where $M := \max\Big\{\int_{\Omega}\Big(S_0(x) + I_{1,0}(x) + I_{2,0}(x)\Big)\, dx, \frac{b^*|\Omega|}{\mu_0}\Big\}$. □

The following lemma establishes a uniform $L^p(\Omega)$-estimate for solutions of system (1.1) for every $2 \leq p < \infty$, which plays a crucial role in the proofs of Theorems 1 and 2.

Lemma 2.2 *Assume that the hypotheses of Lemma 2.1 hold. Then, for every $p \in \mathbb{N}$ with $p \geq 2$, there exists a constant $L_p > 0$, independent of the fractional diffusion order α, such that*

$$\|(S, I_1, I_2)(\cdot, t)\|_{L^p(\Omega)} \leq L_p, \qquad \forall\, t \geq 0.$$

Proof: To establish the $L^p(\Omega)$-estimates, we introduce the following Lyapunov-type functional, which was originally proposed for two-component systems in [30] and later extended to m-component systems in [1]. We assume $u = (u_1, u_2, u_3) \equiv (S, I_1, I_2)$, $\theta = (\theta_1, \theta_2, \theta_3)$, and $a > 0$ (to be determined) to define

$$\mathcal{L}^p(u)(t) = \int_\Omega \sum_{\theta \in \mathbb{Z}^3_+,\ |\theta| = p} \binom{p}{\theta} a^{\sum_{i=1}^3 \theta_i^2} \Pi_{i=1}^3 u_i(x,t)^{\theta_i}\, dx$$

Differentiating with respect to t we get,

$$\begin{aligned}
\mathcal{L}^p(u)'(t) &= \int_\Omega \sum_{|\theta| = p-1} \binom{p}{\theta} a^{\sum_{i=1}^3 \theta_i^2} \Pi_{i=1}^3 u_i(x,t)^{\theta_i} \Big(\sum_{i=1}^3 a^{2\theta_i+1} u_{i_t}(x,t) \Big)\, dx \\
&= \int_\Omega \sum_{|\theta| = p-1} \binom{p}{\theta} a^{\sum_{i=1}^3 \theta_i^2} \Pi_{i=1}^3 u_i(x,t)^{\theta_i} \left(\sum_{i=1}^3 a^{2\theta_i+1} \Big(d_i(-\Delta)^\alpha u_i(x,t) + f_i(x,t,u) \Big) \right) dx \\
&= I + J
\end{aligned} \tag{2.1}$$

where

$$I = \int_\Omega \sum_{|\theta| = p-1} \binom{p}{\theta} a^{\sum_{i=1}^3 \theta_i^2} \Pi_{i=1}^3 u_i(x,t)^{\theta_i} \sum_{i=1}^3 a^{2\theta_i+1} d_i (-\Delta)^\alpha u_i(x,t)\, dx$$

If we consider $K(x,y) = \frac{C_{n,\alpha}}{|x-y|^{n+2\alpha}}$ in (1.3), then we can write,

$$\begin{aligned}
I &= \int_{\Omega\times\Omega} \sum_{|\theta| = p-1} \binom{p}{\theta} a^{\sum_{i=1}^3 \theta_i^2} \Pi_{i=1}^3 u_i(x,t)^{\theta_i} \sum_{i=1}^3 a^{2\theta_i+1} d_i K(x,y)(u_i(y,t) - u_i(x,t))\, dy\, dx \\
&= \int_{\Omega\times\Omega} K(x,y) \sum_{i=1}^3 U_i(v(x,t)) \psi_i(x,y,t)\, dy\, dx \qquad \Big[\psi_i(x,y,t) = u_i(y,t) - u_i(x,t),\ i = 1,2,3\Big]
\end{aligned}$$

where

$$\sum_{i=1}^3 U_i(v(x,t)) = \sum_{|\theta| = p-1} \binom{p}{\theta} a^{\sum_{i=1}^3 \theta_i^2} \Pi_{i=1}^3 u_i(x,t)^{\theta_i} \sum_{i=1}^3 a^{2\theta_i+1} d_i \text{ and } v(\cdot,t) = \Big(S(\cdot,t), I_1(\cdot,t), I_2(\cdot,t)\Big)$$

Due to the fact that $K(x,y) = K(y,x) > 0$, for any $\Theta > 0$ we have

$$\int_{\Omega\times\Omega} v(x,t)^\Theta K(x,y)(v(y,t) - v(x,t))\, dy\, dx = -\frac{1}{2} \int_{\Omega\times\Omega} (v(y,t)^\Theta - v(x,t)^\Theta) K(x,y)(v(y,t) - v(x,t))\, dx\, dy$$

Using this estimate we can write

$$\begin{aligned}
I &= -\frac{1}{2} \int_{\Omega\times\Omega} K(x,y) \sum_{i=1}^3 \Big(U_i(v(y,t)) - U_i(v(x,t)) \Big) \psi_i(x,y,t)\, dy\, dx \\
&= -\frac{1}{2} \int_{\Omega\times\Omega} K(x,y) \Big(U(v(y,t),x,y,t) - U(v(x,t),x,y,t) \Big)\, dy\, dx
\end{aligned}$$

where we used $U(v,x,y,t) = \sum_{i=1}^{3} U_i(v)\psi_i(x,y,t)$. Now, using Mean Value Theorem (differentiating with respect to $\{S, I_1, I_2\}$) we can write

$$\begin{aligned} I &= -\frac{1}{2}\int_{\Omega\times\Omega} K(x,y) \sum_{i\in\{S,I_1,I_2\}} \Big(U_i(\tilde{v}(y,t)x,y,t) - U_i(\tilde{v}(x,t),x,y,t)\Big)\,dy\,dx \\ &= -\frac{1}{2}\int_{\Omega\times\Omega} K(x,y)\Big[U_S(\tilde{v}(x,y,t),x,y,t)\psi_S + U_{I_1}(\tilde{v}(x,y,t),x,y,t)\psi_{I_1} + U_{I_2}(\tilde{v}(x,y,t),x,y,t)\psi_{I_2}\Big]\,dy\,dx \end{aligned} \tag{2.2}$$

where $\tilde{v}(x,y,t) = v(x,t) + \hat{K}(v(x,t),v(y,t),x,y,t)(v(y,t)-v(x,t))$ and $0 < \hat{K}(v(x,t),v(y,t),x,y,t) < 1$. Also, $\psi_i = \psi_i(x,y,t),\ i \in \{S, I_1, I_2\}$. Now,

$$U_S(\tilde{v}(x,y,t),x,y,t) = \frac{\partial}{\partial\tilde{S}}\left(\sum_{i=1}^{3} U_i(\tilde{v})\psi_i\right) = \frac{\partial}{\partial\tilde{S}}\left(\sum_{|\theta|=p-1}\binom{p}{\theta} a^{\sum_{i=1}^{3}\theta_i^2}\Pi_{i=1}^{3}\tilde{u_i}(x,t)^{\theta_i}\sum_{i=1}^{3} a^{2\theta_i+1}d_i\psi_i\right) = a_1 + b_1 + c_1$$

Now,

$$\begin{aligned} a_1 &= \frac{\partial}{\partial\tilde{S}}\left(\sum_{|\theta|=p-1}\binom{p}{\theta} a^{\sum_{i=1}^{3}\theta_i^2}\Pi_{i=1}^{3}\tilde{u_i}(x,t)^{\theta_i} a^{2\theta_1+1}d_S\psi_S\right) \\ &= \sum_{\theta_1+\theta_2+\theta_3=p-1}\binom{p}{\theta_1\ \theta_2\ \theta_3} a^{\theta_1^2+\theta_2^2+\theta_3^2}\theta_1\tilde{S}(x,y,t)^{\theta_1-1}\tilde{I_1}(x,y,t)^{\theta_2}\tilde{I_2}(x,y,t)^{\theta_3}a^{2\theta_1+1}d_S\psi_S(x,y,t) \\ &= \sum_{\theta_1+\theta_2+\theta_3=p-1}\frac{1}{\theta_1!}\binom{p}{\theta_2\ \theta_3} a^{\theta_1^2+\theta_2^2+\theta_3^2}\theta_1\tilde{S}(x,y,t)^{\theta_1-1}\tilde{I_1}(x,y,t)^{\theta_2}\tilde{I_2}(x,y,t)^{\theta_3}a^{2\theta_1+1}d_S\psi_S(x,y,t) \\ &= \sum_{\theta_1+\theta_2+\theta_3=p-1}\frac{1}{(\theta_1-1)!}\binom{p}{\theta_2\ \theta_3} a^{\theta_1^2+\theta_2^2+\theta_3^2}\tilde{S}(x,y,t)^{\theta_1-1}\tilde{I_1}(x,y,t)^{\theta_2}\tilde{I_2}(x,y,t)^{\theta_3}a^{2\theta_1+1}d_S\psi_S(x,y,t) \\ &= \sum_{(\theta_1-1)+\theta_2+\theta_3=p-2}\frac{1}{(\theta_1-1)!}\binom{p}{\theta_2\ \theta_3} a^{(\theta_1-1)^2+\theta_2^2+\theta_3^2}\tilde{S}(x,y,t)^{\theta_1-1}\tilde{I_1}(x,y,t)^{\theta_2}\tilde{I_2}(x,y,t)^{\theta_3}a^{4(\theta_1-1)+4}d_S\psi_S(x,y,t) \\ &= \sum_{\theta_1+\theta_2+\theta_3=p-2}\frac{1}{\theta_1!}\binom{p}{\theta_2\ \theta_3} a^{\theta_1^2+\theta_2^2+\theta_3^2}\tilde{S}(x,y,t)^{\theta_1}\tilde{I_1}(x,y,t)^{\theta_2}\tilde{I_2}(x,y,t)^{\theta_3}a^{4\theta_1+4}d_S\psi_S(x,y,t) \\ &= \sum_{\theta_1+\theta_2+\theta_3=p-2}\binom{p}{\theta_1\ \theta_2\ \theta_3} a^{\theta_1^2+\theta_2^2+\theta_3^2}\tilde{S}(x,y,t)^{\theta_1}\tilde{I_1}(x,y,t)^{\theta_2}\tilde{I_2}(x,y,t)^{\theta_3}a^{4\theta_1+4}d_S\psi_S(x,y,t) \\ &= \sum_{\theta=0}^{p-2}\binom{p}{\theta} a^{\theta_1^2+\theta_2^2+\theta_3^2}\tilde{S}(x,y,t)^{\theta_1}\tilde{I_1}(x,y,t)^{\theta_2}\tilde{I_2}(x,y,t)^{\theta_3}a^{4\theta_1+4}d_S\psi_S(x,y,t) \end{aligned}$$

Using similar technique, we can find b_1, c_1 and similar estimates for $U_{I_1}(\tilde{v}(x,y,t),x,y,t), U_{I_2}(\tilde{v}(x,y,t),x,y,t)$. Then replacing these into (2.2) we can write

$$\begin{aligned} I &= -\frac{1}{2}\int_{\Omega\times\Omega} K(x,y)\Big[(a_1+b_1+c_1)\psi_S + (a_2+b_2+c_2)\psi_{I_1} + (a_3+b_3+c_3)\psi_{I_2}\Big]\,dy\,dx \\ &= -\frac{1}{2}\int_{\Omega\times\Omega} K(x,y)\sum_{|\theta|=p-2}\binom{p}{\theta} a^{\theta_1^2+\theta_2^2+\theta_3^2}\tilde{S}(x,y,t)^{\theta_1}\tilde{I_1}(x,y,t)^{\theta_2}\tilde{I_2}(x,y,t)^{\theta_3}\begin{pmatrix}\psi_S & \psi_{I_1} & \psi_{I_2}\end{pmatrix} \\ &\begin{pmatrix} d_S a^{4\theta_1+4} & \frac{d_S+d_{I_1}}{2}a^{2\theta_1+1}a^{2\theta_2+1} & \frac{d_S+d_{I_2}}{2}a^{2\theta_1+1}a^{2\theta_3+1} \\ \frac{d_S+d_{I_1}}{2}a^{2\theta_1+1}a^{2\theta_2+1} & d_{I_1}a^{4\theta_2+4} & \frac{d_{I_1}+d_{I_2}}{2}a^{2\theta_2+1}a^{2\theta_3+1} \\ \frac{d_S+d_{I_2}}{2}a^{2\theta_1+1}a^{2\theta_3+1} & \frac{d_{I_1}+d_{I_2}}{2}a^{2\theta_2+1}a^{2\theta_3+1} & d_{I_2}a^{4\theta_3+4}\end{pmatrix}\begin{pmatrix}\psi_S\\ \psi_{I_1}\\ \psi_{I_2}\end{pmatrix} dy\,dx. \end{aligned}$$

If $\max\left\{\sqrt{\frac{d_S+d_{I_1}}{2\sqrt{d_S d_{I_1}}}}, \sqrt{\frac{d_{I_1}+d_{I_2}}{2\sqrt{d_{I_1}d_{I_2}}}}\right\} < a < \min\left\{\sqrt{\frac{(d_S+d_{I_1})(d_{I_1}+d_{I_2})}{2d_{I_1}(d_S+d_{I_2})}}, \sqrt{\frac{(d_S+d_{I_2})(d_{I_1}+d_{I_2})}{2d_{I_2}(d_S+d_{I_1})}}\right\}$, then using Sylvester's Criterion we can write the quadratic term in I above as $z^T A z \geq 0\ \forall\ z \in \mathbb{R}^3$ where

$A = \begin{pmatrix} d_S a^{4\theta_1+4} & \frac{d_S+d_{I_1}}{2} a^{2\theta_1+1}a^{2\theta_2+1} & \frac{d_S+d_{I_2}}{2} a^{2\theta_1+1}a^{2\theta_3+1} \\ \frac{d_S+d_{I_1}}{2} a^{2\theta_1+1}a^{2\theta_2+1} & d_{I_1} a^{4\theta_2+4} & \frac{d_{I_1}+d_{I_2}}{2} a^{2\theta_2+1}a^{2\theta_3+1} \\ \frac{d_S+d_{I_2}}{2} a^{2\theta_1+1}a^{2\theta_3+1} & \frac{d_{I_1}+d_{I_2}}{2} a^{2\theta_2+1}a^{2\theta_3+1} & d_{I_2} a^{4\theta_3+4} \end{pmatrix}$ and $z = \psi_i$ for all $i \in \{S, I_1, I_2\}$. Therefore, we have

$$I \leq 0. \tag{2.3}$$

We also have,

$$\begin{aligned} J &= \int_\Omega \sum_{|\theta|=p-1} \binom{p}{\theta} a^{\sum_{i=1}^3 \theta_i^2} \Pi_{i=1}^3 u_i(x,t)^{\theta_i} \left(\sum_{i=1}^3 a^{2\theta_i+1} f_i(x,t,u) \right) dx \\ &= \int_\Omega \sum_{|\theta|=p-1} \binom{p}{\theta} a^{\sum_{i=1}^3 \theta_i^2} \Pi_{i=1}^3 u_i(x,t)^{\theta_i} \Big[(a^{2\theta_1+1} - \sigma(x)a^{2\theta_2+1} + \sigma(x)a^{2\theta_3+1} - a^{2\theta_3+1}) f_1(x,t,u) \\ &+ (a^{2\theta_2+1} - a^{2\theta_3+1}) \Big(\sigma(x) f_1(x,t,u) + f_2(x,t,u) \Big) + a^{2\theta_3+1} \Big(f_1(x,t,u) + f_2(x,t,u) + f_3(x,t,u) \Big) \Big] dx \\ &= J_1 + J_2 + J_3 \end{aligned} \tag{2.4}$$

Since, $\sigma(x) \geq 0$, if $a > 1$ and $\theta_3 < \min\{\theta_1, \theta_2\}$ then $(a^{2\theta_2+1} - a^{2\theta_3+1}) > 0$ and $(a^{2\theta_1+1} - \sigma(x)a^{2\theta_2+1} + \sigma(x)a^{2\theta_3+1} - a^{2\theta_3+1}) > 0$. Now,

$$\begin{aligned} J_1 &= \int_\Omega \sum_{|\theta|=p-1} \binom{p}{\theta} a^{\sum_{i=1}^3 \theta_i^2} \Pi_{i=1}^3 u_i(x,t)^{\theta_i} (a^{2\theta_1+1} - \sigma(x)a^{2\theta_2+1} + \sigma(x)a^{2\theta_3+1} - a^{2\theta_3+1}) f_1(x,t,u)\, dx \\ &= \int_\Omega \sum_{|\theta|=p-1} \binom{p}{\theta} a^{\sum_{i=1}^3 \theta_i^2} \Pi_{i=1}^3 u_i(x,t)^{\theta_i} (a^{2\theta_1+1} - \sigma(x)a^{2\theta_2+1} + \sigma(x)a^{2\theta_3+1} - a^{2\theta_3+1}) \Big(b(x) - g(x,t)S(x,t) - \mu(x)S(x,t) \Big) dx \\ &\leq \int_\Omega \sum_{|\theta|=p-1} \binom{p}{\theta} a^{\sum_{i=1}^3 \theta_i^2} \Pi_{i=1}^3 u_i(x,t)^{\theta_i} dx \Big\| (a^{2\theta_1+1} - \sigma(x)a^{2\theta_2+1} + \sigma(x)a^{2\theta_3+1} - a^{2\theta_3+1}) b(x) \Big\|_{\infty,\Omega} \\ &\leq b^* \sigma_1^* \Big(a^{2\theta_1+1} + a^{2\theta_2+1} + 2a^{2\theta_3+1} \Big) \int_\Omega \sum_{|\theta|=p-1} \binom{p}{\theta} a^{\sum_{i=1}^3 \theta_i^2} \Pi_{i=1}^3 u_i(x,t)^{\theta_i}\, dx \end{aligned}$$

where we used Hölder's inequality, considered $\sigma_1^* = \max\{1, \sigma^*\}$. Using similar technique we get,

$$J_2 \leq b^* \sigma^* (a^{2\theta_2+1} - a^{2\theta_3+1}) \int_\Omega \sum_{|\theta|=p-1} \binom{p}{\theta} a^{\sum_{i=1}^3 \theta_i^2} \Pi_{i=1}^3 u_i(x,t)^{\theta_i}\, dx$$

and

$$\begin{aligned} J_3 &\leq \int_\Omega \sum_{|\theta|=p-1} \binom{p}{\theta} a^{\sum_{i=1}^3 \theta_i^2} \Pi_{i=1}^3 u_i(x,t)^{\theta_i} a^{2\theta_3+1} \Big(b(x) - \mu(x) \sum_{i=1}^3 u_i(x,t) \Big) dx \\ &\leq b^* a^{2\theta_3+1} \int_\Omega \sum_{|\theta|=p-1} \binom{p}{\theta} a^{\sum_{i=1}^3 \theta_i^2} \Pi_{i=1}^3 u_i(x,t)^{\theta_i}\, dx - \mu_0 a^{2\theta_3+1} \int_\Omega \sum_{|\theta|=p-1} \binom{p}{\theta} a^{\sum_{i=1}^3 \theta_i^2} \Pi_{i=1}^3 u_i(x,t)^{\theta_i} \sum_{i=1}^3 u_i(x,t)\, dx \\ &\leq b^* a^{2\theta_3+1} \int_\Omega \sum_{|\theta|=p-1} \binom{p}{\theta} a^{\sum_{i=1}^3 \theta_i^2} \Pi_{i=1}^3 u_i(x,t)^{\theta_i}\, dx - a^{2\theta_3+1} \mu_0 p! \int_\Omega \sum_{|\theta|=p} \binom{p}{\theta} a^{\sum_{i=1}^3 \theta_i^2} \Pi_{i=1}^3 u_i(x,t)^{\theta_i}\, dx \end{aligned}$$

Replacing J_1, J_2, J_3 in (2.4) we get,

$$\begin{aligned} J \leq \Big[b^* \sigma_1^* \Big(a^{2\theta_1+1} + a^{2\theta_2+1} + 2a^{2\theta_3+1} \Big) + b^* \sigma^* (a^{2\theta_2+1} - a^{2\theta_3+1}) + b^* a^{2\theta_3+1} \Big] \int_\Omega \sum_{|\theta|=p-1} \binom{p}{\theta} a^{\sum_{i=1}^3 \theta_i^2} \\ \Pi_{i=1}^3 u_i(x,t)^{\theta_i}\, dx - a^{2\theta_3+1} \mu_0 p! \int_\Omega \sum_{|\theta|=p} \binom{p}{\theta} a^{\sum_{i=1}^3 \theta_i^2} \Pi_{i=1}^3 u_i(x,t)^{\theta_i}\, dx \end{aligned}$$

$$\leq C_1 \int_\Omega \sum_{|\theta|=p-1} \binom{p}{\theta} a^{\sum_{i=1}^3 \theta_i^2} \Pi_{i=1}^3 u_i(x,t)^{\theta_i}\, dx - a^{2\theta_3+1}\mu_0 p! \int_\Omega \sum_{|\theta|=p} \binom{p}{\theta} a^{\sum_{i=1}^3 \theta_i^2} \Pi_{i=1}^3 u_i(x,t)^{\theta_i}\, dx$$

Since $a > 1$, $\max\left\{ \sqrt{\frac{d_S+d_{I_1}}{2\sqrt{d_S d_{I_1}}}}, \sqrt{\frac{d_{I_1}+d_{I_2}}{2\sqrt{d_{I_1} d_{I_2}}}} \right\} < a < \min\left\{ \sqrt{\frac{(d_S+d_{I_1})(d_{I_1}+d_{I_2})}{2d_{I_1}(d_S+d_{I_2})}}, \sqrt{\frac{(d_S+d_{I_2})(d_{I_1}+d_{I_2})}{2d_{I_2}(d_S+d_{I_1})}} \right\}$, $\theta_3 < \min\{\theta_1, \theta_2\}$, and by considering $a \geq 1$ we can write,

$$\mathcal{L}^p(u)(t) = \int_\Omega \sum_{|\theta|=p} \binom{p}{\theta} a^{\sum_{i=1}^3 \theta_i^2} \Pi_{i=1}^3 u_i(x,t)^{\theta_i}\, dx \leq \max\{a\} \int_\Omega \sum_{|\theta|=p} \binom{p}{\theta} \Pi_{i=1}^3 u_i(x,t)^{\theta_i}\, dx.$$

So, if, $\max\left\{1, \sqrt{\frac{d_S+d_{I_1}}{2\sqrt{d_S d_{I_1}}}}, \sqrt{\frac{d_{I_1}+d_{I_2}}{2\sqrt{d_{I_1} d_{I_2}}}} \right\} < a < \min\left\{ \sqrt{\frac{(d_S+d_{I_1})(d_{I_1}+d_{I_2})}{2d_{I_1}(d_S+d_{I_2})}}, \sqrt{\frac{(d_S+d_{I_2})(d_{I_1}+d_{I_2})}{2d_{I_2}(d_S+d_{I_1})}} \right\}$, and $\theta_3 < \min\{\theta_1, \theta_2\}$, then we get,

$$\begin{aligned} J &\leq C_1 \mathcal{L}^{p-1}(u)(t) - \frac{p! a^{2\theta_3+1}\mu_0}{\max\{a\}} \mathcal{L}^p(u)(t) \\ &\leq C_1 \mathcal{L}^{p-1}(u)(t) - C_2 \mathcal{L}^p(u)(t) \end{aligned}$$

Replacing I and J in (2.1) we get,

$$\begin{aligned} \mathcal{L}^p(u)'(t) &\leq -I + C_1 \mathcal{L}^{p-1}(u)(t) - C_2 \mathcal{L}^p(u)(t) \\ &\leq C_1 \mathcal{L}^{p-1}(u)(t) - C_2 \mathcal{L}^p(u)(t) \end{aligned} \tag{2.5}$$

Taking $p = 2$ we get,

$$\mathcal{L}^2(u)'(t) + C_2 \mathcal{L}^p(u)(t) \leq C_1 \mathcal{L}^1(u)(t) \leq C_1 M \qquad \text{(using Lemma 2.1)}$$

using Grönwall's inequality we get,

$$\mathcal{L}^2(u)(t) \leq M_2, \quad \forall\, t \in [0, T_m) \text{ and for any } M_2 > 0.$$

Proceeding inductively by taking $p = 3, 4, \ldots$ in (2.5), we conclude that for every $t \geq 0$ and each $2 \leq p < \infty$, there exists a constant $M_p > 0$ such that

$$\mathcal{L}^p(u)(t) \leq M_p.$$

Moreover, since $\theta \in (0, \infty)^3$, there exist positive constants ε_1 and ε_2, depending only on θ, such that

$$\varepsilon_1 \|u(\cdot,t)\|_{L^p(\Omega)} \leq \left(\mathcal{L}^p(u)(t)\right)^{\frac{1}{p}} \leq \varepsilon_2 \|u(\cdot,t)\|_{L^p(\Omega)}, \qquad 2 \leq p < \infty.$$

Hence,

$$\|u(\cdot,t)\|_{L^p(\Omega)} \leq L_p, \qquad \forall\, t \geq 0,\ 2 \leq p < \infty,$$

for some constant $L_p > 0$. □

Proof of Theorem 1: With the above setting before Lemma (2.1), standard semilinear evolution theory [43] guarantees that system (1.1) admits a unique maximal solution $(S, I_1, I_2) \in C([0, T_m); \mathbb{X})$, defined on a maximal interval $[0, T_m)$, where $T_m \in (0, \infty]$. Moreover, the solution satisfies the variation-of-constants formulas

$$u(x,t) = T_u(t)u_0(x) + \int_0^t T_u(t-\tau) F(x, \tau, S, I_1, I_2, R) d\tau,$$

for $u \in \{S, I_1, I_2\}, F = f_i$. Since the reaction terms satisfy the quasi-positivity condition (Qp), standard comparison arguments along with nonnegative initial data imply that the maximal solution remains component-wise nonnegative. Thus,

$$S(x,t) \geq 0, \qquad I_1(x,t) \geq 0, \qquad I_2(x,t) \geq 0,$$

for all $x \in \Omega$ and $t \in [0, T_m)$.

To establish global existence, it suffices to rule out finite-time blow-up. More precisely, the continuation principle implies that either $T_m = \infty$ or

$$\limsup_{t \to T_m^-} \left\{ \|S(\cdot,t)\|_{\infty,\Omega} + \|I_1(\cdot,t)\|_{\infty,\Omega} + \|I_2(\cdot,t)\|_{\infty,\Omega} \right\} = \infty. \tag{2.6}$$

Consequently, global existence follows once it is shown that the solution remains uniformly bounded in $L^\infty(\Omega)$ on every finite time interval.

Now, if we define $A_{SS}(z) = d_S(-\Delta)^\alpha z - \mu_0 z$, then $A_{SS}(z)$ generates $T_{SS}(t)$ on $L^2(\Omega)$. Also, since S, I_1, I_2 are nonnegative then the first equation of (1.1) yields

$$\begin{aligned} S_t(x,t) &= d_S(-\Delta)^\alpha S(x,t) + b(x) - g(x,t)S(x,t) - \mu(x)S(x,t) \\ &\leq d_S(-\Delta)^\alpha S(x,t) + b^* - \mu_0 S(x,t) \end{aligned}$$

which gives us

$$S(x,t) \leq T_{SS}(t)S_0(x) + b^* \int_0^t T_{SS}(t-\tau)\, d\tau \leq \|T_{SS}(t)S_0\|_{\infty,\Omega} + b^* \int_0^t \|T_{SS}(t-\tau)\|_{\infty,\Omega}\, d\tau$$

Hence,

$$\|S(\cdot,t)\|_{\infty,\Omega} \leq C_3, \quad t > 0 \tag{2.7}$$

where $C_3 := \max\left\{ \|S_0\|_{\infty,\Omega}, \frac{b^*}{\mu_0} \right\}$. We now invoke Lemma 2.1 and 2.2, which provide the $L^1(\Omega)$ and $L^p(\Omega)$ estimates, respectively for infected class I_1, I_2, for $0 \leq \tau < T < T_m$. Integrating the $L^p(\Omega)$ estimates of I_1, I_2 in Lemma 2.2 with respect to time from τ to T, we can write

$$\|I_1\|_{p,\Omega\times(\tau,T)}, \|I_2\|_{p,\Omega\times(\tau,T)} \leq L_p(T-\tau) \tag{2.8}$$

for $2 \leq p < \infty$.

Note that since this estimate only depends on the size of $T - \tau$, it follows from a limiting process that

$$\|I_1\|_{p,\Omega\times(\tau,T_m)}, \|I_2\|_{p,\Omega\times(\tau,T_m)} \leq L_p(T_m-\tau). \tag{2.9}$$

Since, $g(x,t) \geq 0$, let us recall that

$$\begin{aligned} f_2(x,t,S,I_1,I_2,R) &= \sigma(x)g(x,t)S(x,t) - \Big(\lambda_1(x) + \mu(x)\Big)I_1(x,t) \leq \sigma(x)g(x,t)S(x,t) \leq \sigma^* g(x,t)S(x,t) \\ f_3(x,t,S,I_1,I_2,R) &= \Big(1-\sigma(x)\Big)g(x,t)S(x,t) - \Big(\lambda_2(x) + \mu(x) + \delta(x) + \gamma(x,t)\Big)I_2(x,t) \leq g(x,t)S(x,t) \end{aligned}$$

so, if we define

$$G(x,t) = \sigma_1^* g(x,t)S(x,t)$$

where $\sigma_1^* = \max\left\{1, \sigma^*\right\}$, then

$$f_j(x,t) \leq G(x,t), \quad \text{for } j = 2,3.$$

Then (2.9), Lemma 2.1 and (2.7) imply the boundedness of $\|G(\cdot,t)\|_{p,\Omega\times(\tau,T_m)}$ for each $1 \leq p < \infty$. For $j = 1, 2$ let Ψ_j be the unique nonnegative solution to

$$\begin{cases} \Psi_{j_t}(x,t) & = d_j(-\Delta)^\alpha \Psi_j(x,t) + G(x,t), \Omega \times (0,T_m), \\ \mathcal{N}_\alpha \Psi & = 0, \qquad\qquad \mathbb{R}^n \setminus \Omega \times (0,T_m), \\ \Psi_j & = I_{j,0}(x), \qquad\qquad \Omega \times \{0\}, \end{cases}$$

Then comparison principle for fractional parabolic initial boundary value problems implies that $I_j \le \Psi_j$ for $j = 1, 2$ and from the $L^p(\Omega \times (0, T_m))$ bound on $G(x,t)$ for $p > \frac{n+2\alpha}{2\alpha}$, $\|\Psi_j\|_{\infty,\Omega\times(0,T_m)}$ is bounded for $j = 1, 2$. Therefore, $\|I_1\|_{\infty,\Omega\times(\tau,T_m)}\|I_2\|_{\infty,\Omega\times(\tau,T_m)}$ is bounded. So, there exists a constant $C_4 > 0$ such that

$$\|I_1(\cdot,t)\|_{L^\infty(\Omega)}, \|I_2(\cdot,t)\|_{L^\infty(\Omega)} \le C_4 \qquad \text{for all } t > 0, \tag{2.10}$$

where C_4 depends on $\|S_0\|_{L^\infty(\Omega)}$, $\|I_{1,0}\|_{L^\infty(\Omega)}$, $\|I_{2,0}\|_{L^\infty(\Omega)}$, $d_S, d_{I_1}, d_{I_2}, \mu_0, \lambda_0, \delta_0, \gamma_0, b^*, C_{n,\alpha}, \sigma_1^*, \beta^*, \alpha$, and the domain Ω, but is independent of time. This along with (2.7) proves the theorem. □

The following result is analogous to Lemma 2.1; however, its proof relies essentially on the nonlocal nature of the infection incidence term. It is worth noting that, during the treatment-free intervals, the treatment rate satisfies $\gamma(x,t) = 0$, and consequently the corresponding estimates reduce to those of the treatment-free case.

Lemma 2.3 *Assume that the hypotheses of Theorem 1 and Lemma 2.2 hold. If* $\xi = \min\left\{\lambda_{1,0}+\mu_0, \lambda_{2,0}+\mu_0+\delta_0+\gamma_0\right\} > C_3\zeta$ *where* $\zeta = \max\left\{\Lambda(1+\kappa C^*)\beta_1^*, \beta_2^*\right\}$ *then*

$$\lim_{T\to\infty} \int_T^{T+1} \int_\Omega \Big(I_1(x,t) + I_2(x,t)\Big)\, dx\, dt = 0.$$

Moreover, for every $1 \le q < \infty$,

$$\|I_j\|_{L^q(\Omega\times(T,T+1))} \to 0 \qquad \text{as } T \to \infty, \quad j = 1, 2.$$

Proof: Let $u = (u_1, u_2) \equiv (I_1, I_2)$. If we add the second and third equations of system (1.1) and then integrating over Ω we get,

$$\begin{aligned}
\int_\Omega \sum_{i=1}^{2} u_{i_t}(x,t)\, dx &= \int_\Omega \sum_{i=1}^{2} d_i(-\Delta)^\alpha u_i(x,t)\, dx + \int_\Omega g(x,t)S(x,t)\, dx - \int_\Omega \Big(\lambda_1(x) + \mu(x)\Big)u_1(x,t)\, dx \\
&\quad - \int_\Omega \Big(\lambda_2(x) + \mu(x) + \delta(x) + \gamma(x,t)\Big)u_2(x,t)\, dx \\
&\le C_3 \int_\Omega g(x,t)\, dx - (\lambda_{1,0} + \mu_0) \int_\Omega u_1(x,t)\, dx - (\lambda_{2,0} + \mu_0 + \delta_0 + \gamma_0) \int_\Omega u_2(x,t)\, dx \\
&\le C_3 \int_\Omega g(x,t)\, dx - \xi \int_\Omega \sum_{i=1}^{2} u_i(x,t)\, dx
\end{aligned}$$

where we considered $\xi = \min\left\{\lambda_{1,0} + \mu_0, \lambda_{2,0} + \mu_0 + \delta_0 + \gamma_0\right\}$ which implies $-(\lambda_{1,0} + \lambda_{2,0} + \mu_0 + \delta_0 + \gamma_0) \le -\xi$. Additionally, using the definition of the nonlocal infection incidence term we get

$$\int_\Omega g(x,t)\, dx = \int_\Omega \int_\Omega \rho(x,y)\omega(y)\beta_1(y)I_1(y,t)\, dy\, dx + \int_\Omega \beta_2(x)I_2(x,t)\, dx$$

using Fubini's Theorem on the first term we can write

$$\begin{aligned}
\int_\Omega g(x,t)\, dx &= \left(\int_\Omega \rho(x,y)\, dx\right)\left(\int_\Omega \omega(y)\beta_1(y)I_1(y,t)\, dy\right) + \int_\Omega \beta_2(x)I_2(x,t)\, dx \\
&\le \Lambda \int_\Omega \omega(y)\beta_1(y)I_1(y,t)\, dy + \int_\Omega \beta_2(x)I_2(x,t)\, dx \\
&\le \Lambda\omega^*\beta_1^* \int_\Omega I_1(x,t)\, dx + \beta_2^* \int_\Omega I_2(x,t)\, dx = \Lambda(1+\kappa C^*)\beta_1^* \int_\Omega I_1(x,t)\, dx + \beta_2^* \int_\Omega I_2(x,t)\, dx \\
&\le \zeta \int_\Omega \Big(I_1(x,t) + I_2(x,t)\Big)\, dx = \zeta \int_\Omega \sum_{i=1}^{2} u_i(x,t)\, dx
\end{aligned}$$

where $\zeta = \max\left\{\Lambda(1+\kappa C^*)\beta_1^*, \beta_2^*\right\}$. Replacing this along with ξ we get,

$$\int_\Omega \sum_{i=1}^{2} u_{i_t}(x,t)\,dx \le C_3\zeta \int_\Omega \sum_{i=1}^{2} u_i(x,t)\,dx - \xi \int_\Omega \sum_{i=1}^{2} u_i(x,t)\,dx \tag{2.11}$$

for $\xi > C_3\zeta$, we solve the above differential inequality and then integrate with respect to time from T to $T+1$ to get

$$\lim_{T\to\infty} \int_T^{T+1} \int_\Omega \sum_{i=1}^{2} u_i(x,t)\,dx\,dt = \lim_{T\to\infty} \int_T^{T+1} \int_\Omega \Big(I_1(x,t) + I_2(x,t)\Big)\,dx\,dt = 0. \tag{2.12}$$

Now, by virtue of Lemma 2.2, the infected populations I_1 and I_2 are uniformly bounded in $L^p(\Omega)$ for every $1 < p < \infty$. Integrating the estimate of Lemma 2.2 over the time interval $(T, T+1)$, we obtain

$$\|I_j\|_{L^p(\Omega\times(T,T+1))} \le C_p, \qquad \forall\, T \ge 0, \quad 1 < p < \infty, \quad j = 1,2, \tag{2.13}$$

where $C_p > 0$ is independent of T.

Let $q > 1$. Since

$$I_j^q = I_j^{\frac{1}{2}} I_j^{q-\frac{1}{2}},$$

Hölder's inequality yields

$$\int_T^{T+1} \int_\Omega I_j(x,t)^q\,dx\,dt \le \left(\int_T^{T+1} \int_\Omega I_j(x,t)\,dx\,dt\right)^{\frac{1}{2}} \left(\int_T^{T+1} \int_\Omega I_j(x,t)^{2q-1}\,dx\,dt\right)^{\frac{1}{2}},$$

for $j = 1,2$.

Combining (2.12), (2.13), and the nonnegativity of I_j, we infer that

$$\int_T^{T+1} \int_\Omega I_j(x,t)^q\,dx\,dt \longrightarrow 0 \qquad \text{as } T \to \infty.$$

Consequently,

$$\|I_j\|_{L^q(\Omega\times(T,T+1))} \longrightarrow 0 \qquad \text{as } T \to \infty, \quad j = 1,2, \quad 1 \le q < \infty. \tag{2.14}$$

This completes the proof. □

Now, we assume S^* is the disease-free steady state which is the unique positive solution of

$$\begin{cases} d_S(-\Delta)^\alpha S^*(x) + b(x) - \mu(x)S^*(x) = 0, & x \in \Omega, \\ \mathcal{N}_\alpha S^* = 0, & x \in \mathbb{R}^n \setminus \Omega. \end{cases} \tag{2.15}$$

Since $b(x) \ge 0$, $b \not\equiv 0$, and $\mu(x) \ge \mu_0 > 0$, it follows from the positivity of the resolvent associated with $d_S(-\Delta)^\alpha - \mu(x)$ that

$$S^*(x) > 0 \qquad \text{for all } x \in \Omega.$$

Lemma 2.4 *Assume that the hypotheses of Theorem 1 hold and that the condition of Lemma 2.3 is satisfied. If $S_0(x) \le S^*(x)$ in Ω for any S^* satisfying* (2.15)*, then the susceptible population converges to the disease-free steady state S^* on sliding time intervals. More precisely,*

$$\|S - S^*\|_{q,\Omega\times(T,T+1)} \to 0 \qquad \textit{as } T \to \infty,$$

for every $1 \le q < \infty$.

Proof: We assume $S^*(x)$ is the disease-free steady state satisfying (2.15). Now, from the first equation of system (1.1) we can write,

$$0 = d_S(-\Delta)^\alpha S^*(x) + b(x) - \mu(x)S^*(x), \quad x \in \Omega$$

Since, $b(x) \in C(\overline{\Omega})$, $S^* \in L^\infty(\Omega)$ for all $x \in \Omega$ and we define

$$z(x,t) = S^*(x) - S(x,t) \text{ with } z(x,0) = S^*(x) - S(x,0) = S^*(x) - S_0(x) \geq 0.$$

Since S^* is independent of t, then using the first equation of the system (1.1), we get,

$$\begin{aligned} z_t(x,t) &= -S_t(x,t) = -d_S(-\Delta)^\alpha S(x,t) - b(x) + \mu(x)S(x,t) + g(x,t)S(x,t) \\ &= -d_S(-\Delta)^\alpha S(x,t) + d_S(-\Delta)^\alpha S^*(x) - \mu(x)S^*(x) + \mu(x)S(x,t) + g(x,t)S(x,t) \\ &= d_S(-\Delta)^\alpha (S^*(x) - S(x,t)) - \mu(x)(S^*(x) - S(x,t)) + g(x,t)S(x,t) \\ &= d_S(-\Delta)^\alpha z(x,t) - \mu(x)z(x,t) + g(x,t)S(x,t) \end{aligned}$$

Since $z(x,0) \geq 0$ along with $S, I_1, I_2, \beta_1, \beta_2, \rho, \mu, \omega, \kappa, C \geq 0$, and the semigroup generated by $d_S(-\Delta)^\alpha - \mu(x)$ is positive, the comparison principle gives

$$z(x,t) \geq 0 \qquad \text{for all } x \in \Omega,\ t \geq 0.$$

Hence,

$$S(x,t) \leq S^*(x) \qquad \text{for all } x \in \Omega,\ t \geq 0.$$

Now integrate the equation for z over Ω to obtain

$$\begin{aligned} \frac{d}{dt}\int_\Omega z(x,t)\,dx &= d_S \int_\Omega (-\Delta)^\alpha z(x,t)\,dx - \int_\Omega \mu(x)z(x,t)\,dx + \int_\Omega g(x,t)S(x,t)\,dx \\ &\leq -\mu_0 \int_\Omega z(x,t)\,dx + C_3\zeta \int_\Omega \Big(I_1(x,t) + I_2(x,t)\Big)\,dx \end{aligned}$$

If we consider

$$Z(t) = \int_\Omega z(x,t)\,dx = \int_\Omega \Big(S^*(x) - S(x,t)\Big)\,dx$$

then for $\xi > C_3\zeta$, using the estimate obtained from (2.11) (i.e. $\int_\Omega \Big(I_1(x,t) + I_2(x,t)\Big)\,dx \leq e^{-(\xi - C_3\zeta)t}\int_\Omega \Big(I_{1,0}(x) + I_{2,0}(x)\Big)\,dx$) we can write,

$$Z'(t) + \mu_0 Z(t) \leq C_3\zeta e^{-(\xi - C_3\zeta)t}\int_\Omega \Big(I_{1,0}(x) + I_{2,0}(x)\Big)\,dx$$

Since $(\xi - C_3\zeta) > 0$ and $\mu_0 > 0$, multiplying the above inequality by $e^{\mu_0 t}$, integrating from 0 to t, and sending $t \to \infty$, we get

$$Z(t) \to 0.$$

Additionally, $Z(x,t) \geq 0$, therefore, we have

$$\|S(\cdot,t) - S^*\|_{1,\Omega} = \int_\Omega |S(x,t) - S^*(x)|\,dx = \int_\Omega Z(x,t)\,dx = Z(t).$$

Consequently,

$$\int_T^{T+1}\int_\Omega |S(x,t) - S^*(x)|\,dx\,dt = \int_T^{T+1} Z(t)\,dt \to 0, \qquad \text{as } T \to \infty. \tag{2.16}$$

Now, since S is uniformly bounded by (2.7) and $S^* \in L^\infty(\Omega)$, Ω is bounded, it follows for every $1 \le p < \infty$ there exists $C_p^* > 0$ such that

$$\|S - S^*\|_{p,\Omega\times(T,T+1)} \le \|S\|_{p,\Omega\times(T,T+1)} + \|S^*\|_{p,\Omega\times(T,T+1)} \le C_p^*, \qquad \forall\, T \ge 0$$

Using the above estimate along with (2.16) and following the same interpolation argument as in Lemma 2.3, we get

$$\|S - S^*\|_{q,\Omega\times(T,T+1)} \to 0 \qquad \text{as } T \to \infty,$$

for every $1 \le q < \infty$. □

Proof of Theorem 2: By Theorem 1, the solution is global, nonnegative, and uniformly bounded in $L^\infty(\Omega)$. Moreover, by Lemma 2.3, for every $1 \le p < \infty$,

$$\|I_j\|_{L^p(\Omega\times(T,T+1))} \to 0 \qquad \text{as } T \to \infty, \qquad j = 1, 2.$$

Since S is uniformly bounded in $L^\infty(\Omega)$, we obtain

$$\|f_2\|_{L^p(\Omega\times(T,T+1))} \le \sigma^* C_3 \zeta^* \left(\|I_1\|_{L^p(\Omega\times(T,T+1))} + \|I_2\|_{L^p(\Omega\times(T,T+1))}\right) + (\lambda_1^* + \mu^*)\|I_1\|_{L^p(\Omega\times(T,T+1))} \to 0$$

$$\|f_3\|_{L^p(\Omega\times(T,T+1))} \le \sigma_1^* C_3 \zeta^* \left(\|I_1\|_{L^p(\Omega\times(T,T+1))} + \|I_2\|_{L^p(\Omega\times(T,T+1))}\right) + (\lambda_2^* + \mu^* + \delta^* + \gamma^*)\|I_2\|_{L^p(\Omega\times(T,T+1))} \to 0$$

as $T \to \infty$, where we used $\zeta^* = \max\left\{\Lambda^*(1 + \kappa C^*)\beta_1^*|\Omega|, \beta_2^*\right\}$, $\sigma_1^* = \max\left\{1, \sigma\right\}$ and $\Lambda^* = \max_{(x,y)\in(\overline{\Omega}\times\overline{\Omega})}\left\{\rho(x,y)\right\}$ (by the definition of ρ). Hence,

$$\|f_j\|_{L^p(\Omega\times(T,T+1))} \to 0, \qquad \text{as } T \to \infty, \qquad j = 2, 3.$$

By the L^p-regularity theory for fractional parabolic equations with homogeneous nonlocal Neumann boundary conditions, there exists a constant $K_p > 0$, independent of T, such that

$$\|I_j\|_{L^p(T,T+1;W^{2\alpha,p}(\Omega))} + \|\partial_t I_j\|_{L^p(\Omega\times(T,T+1))} \le K_p, \qquad j = 1, 2.$$

Equivalently, I_j is uniformly bounded in the fractional parabolic space

$$W_p^{2\alpha,1}(\Omega \times (T, T+1)).$$

Choose $p > \frac{n+2\alpha}{2\alpha}$. Then the fractional parabolic Sobolev embedding yields

$$W_p^{2\alpha,1}(\Omega \times (T, T+1)) \hookrightarrow C^{\epsilon,\epsilon/(2\alpha)}(\overline{\Omega} \times [T, T+1])$$

for some $\epsilon \in (0, 1)$ [36, 48]. Hence I_1 and I_2 are uniformly Hölder continuous on $\overline{\Omega} \times [T, T+1]$, with Hölder constants independent of T.

Combining this uniform Hölder continuity with the decay of the L^p-norms on sliding time intervals, and applying the standard contradiction argument as in [20], we obtain

$$\lim_{t\to\infty} \|I_j(\cdot, t)\|_{L^\infty(\Omega)} = 0, \qquad j = 1, 2.$$

Now, let S^* denote the disease-free steady state as in Lemma 2.4, and define

$$z(x, t) := S^*(x) - S(x, t)$$

then using Lemma 2.4, for every $1 \le p < \infty$ we have

$$\|z\|_{L^p(\Omega\times(T,T+1))} \to 0 \qquad \text{as } T \to \infty.$$

Following similar argument as above, we obtain

$$\|z(\cdot, t)\|_{\infty,\Omega} \to 0 \qquad \text{as } t \to \infty.$$

Since $z = S^* - S$, it follows that

$$\lim_{t\to\infty} \|S(\cdot, t) - S^*\|_{\infty,\Omega} = 0.$$

□

3 Numerical Simulations

The purpose of this section is to complement the theoretical results established in the previous section through numerical experiments. Rather than providing additional mathematical proofs, these simulations are intended to visualize the effects of regional fractional diffusion, nonlocal asymptomatic transmission, intermittent treatment, and population crowding on disease dynamics.

All simulations are performed on the square domain $\Omega = (0,10)\times(0,10)$, using a uniform 128×128 spatial mesh over the time interval $[0,200]$. Time integration is carried out using an implicit–explicit second-order backward differentiation formula (IMEX–BDF2), in which the diffusion operators are treated implicitly while the nonlinear reaction terms are handled explicitly.

The regional fractional Laplacian in each compartment is discretized through the Riesz integral representation. For a generic variable $U \in \{S, I_1, I_2, R\}$,

$$(-\Delta)^{\alpha} U(x_i, y_j) \approx C_{n,\alpha} \sum_{\substack{(k,\ell)\neq(i,j)\\(x_k,y_\ell)\in\Omega}} \frac{U_{i,j} - U_{k,\ell}}{\left[(x_i - x_k)^2 + (y_j - y_\ell)^2\right]^{\frac{n+2\alpha}{2}}} \Delta x\, \Delta y, \tag{3.1}$$

the interactions are restricted to the computational domain, consistent with the homogeneous nonlocal boundary condition (1.2) and the regional fractional Laplacian (1.3).

The nonlocal incidence term associated with the asymptomatic infected population is evaluated using the two-dimensional Gaussian kernel with unit variance,

$$\rho(x,y) = \frac{1}{2\pi} \exp\!\left(-\frac{|x-y|^2}{2}\right).$$

The resulting semi-discrete system is advanced in time using a second-order IMEX–BDF2 scheme, where the fractional diffusion terms are treated implicitly and the nonlinear reaction and nonlocal incidence terms explicitly.

The diffusion coefficients, initial conditions, and spatially heterogeneous coefficient functions used in the numerical simulations are summarized in Table 2.

Table 2: Initial conditions and spatially heterogeneous coefficient functions used in the numerical simulations.

Quantity	Spatial form	Quantity	Spatial form
d_S	0.10	d_{I_1}	0.06
d_{I_2}	0.045	d_R	0.05
$S(x,y,0)$	$100\Big(1 + 0.20\cos\frac{\pi x}{L_x}\cos\frac{\pi y}{L_y}\Big)$	$b(x,y)$	$0.25\Big(0.55 + 0.45\cos^2\frac{\pi x}{L_x}\cos^2\frac{\pi y}{L_y}\Big)$
$I_1(x,y,0)$	$0.90\Big(1 + 0.65e^{-\frac{(x-5)^2+(y-5)^2}{2.5}}\Big)$	$\beta_1(x,y)$	$0.0055(0.35 + 0.65\mathcal{R}(x,y))$
$I_2(x,y,0)$	$0.35\Big(1 + 0.80e^{-\frac{(x-3)^2+(y-7)^2}{1.8}}\Big)$	$\beta_2(x,y)$	$0.0035\Big(0.45 + 0.55\phi_2(x,y)\Big)$
$R(x,y,0)$	0	$\sigma(x,y)$	$0.68\Big(0.90 + 0.10\phi_1(x,y)\Big)$
$\mu(x,y)$	$0.010\Big(0.80 + 0.40\cos^2\frac{\pi x}{L_x}\cos^2\frac{\pi y}{L_y}\Big)$	$\lambda_1(x,y)$	$0.055\Big(0.80 + 0.40\phi_1(x,y)\Big)$

Continued on next page

Table 2: Initial conditions and spatially heterogeneous coefficient functions used in the numerical simulations (continued).

Quantity	Spatial form	Quantity	Spatial form
$\lambda_2(x,y)$	$0.040\Big(0.80 + 0.40\phi_2(x,y)\Big)$	$\delta(x,y)$	$0.012\Big(0.75 + 0.50\phi_3(x,y)\Big)$
$\phi_1(x,y)$	$\sin\Big(\frac{\pi x}{L_x}\Big)\sin\Big(\frac{\pi y}{L_y}\Big)$	$\phi_2(x,y)$	$\exp\Big(-\frac{(x-7)^2+(y-3)^2}{5}\Big)$
$\phi_3(x,y)$	$\exp\Big(-\frac{(x-3)^2+(y-7)^2}{3}\Big)$	$\gamma_1(x,y)$	$0.055\Big(0.70 + 0.80\phi_1 + 0.40\phi_2\Big)$
$C(x,y)$	$1 + \sin^2\Big(\frac{\pi x}{L_x}\Big)\sin^2\Big(\frac{\pi y}{L_y}\Big)$		
κ	0.40	$\omega(x,y)$	$1 + \kappa C(x,y) =$ $1.40 + 0.40\sin^2\Big(\frac{\pi x}{L_x}\Big)\sin^2\Big(\frac{\pi y}{L_y}\Big)$

where

$$\mathcal{R}(x,y) = \frac{0.50\,\phi_1(x,y) + 0.30\,\phi_2(x,y) + 0.20\,\phi_3(x,y)}{\max\limits_{(x,y)\in\Omega}\Big(0.50\,\phi_1(x,y) + 0.30\,\phi_2(x,y) + 0.20\,\phi_3(x,y)\Big)}.$$

which denotes a spatial risk function constructed as a weighted combination of the three basis functions $\phi_1(x,y)$, $\phi_2(x,y)$, and $\phi_3(x,y)$. The function $\phi_1(x,y)$ represents a smooth large-scale spatial variation across the computational domain, whereas $\phi_2(x,y)$ and $\phi_3(x,y)$ represent localized Gaussian hotspots that model regions of elevated epidemiological activity. The weighted combination $\mathcal{R}(x,y)$ is used to generate the spatial heterogeneity in the transmission-related coefficients while maintaining their prescribed average magnitudes and ensuring that the coefficients remain uniformly bounded over the spatial domain.

Throughout the simulations, treatment is applied only to the symptomatic infected class I_2. The intermittent treatment function is prescribed by

$$\gamma(x,y,t) = \begin{cases} 0, & kT_\gamma \le t < (k+1)T_\gamma - L_\gamma, \\ \gamma_1(x,y), & (k+1)T_\gamma - L_\gamma \le t < (k+1)T_\gamma, \end{cases} \qquad k = 0,1,2,\ldots.$$

In the numerical simulations, we take $T_\gamma = 20$, $L_\gamma = 15$. Thus, treatment is inactive during the first 5 time units of each intervention cycle and active during the final 15 time units, corresponding to a 75% duty cycle. The treatment coefficient satisfies $0 \le \gamma_1(x,y) < \gamma_0$, where the upper bound is chosen as $\gamma_0 = 0.33$. The treatment function appears only in the symptomatic infected and recovered equations, so that symptomatic individuals removed through treatment are transferred directly to the recovered class. No treatment term is included in the asymptomatic infected equation; consequently, the I_1 population is influenced only indirectly through the nonlocal force of infection. The periodic on–off protocol represents intermittent treatment strategies arising from scheduled intervention campaigns, temporary treatment availability, limited medical resources, or periodic public health measures. The spatial dependence of $\gamma_1(x,y)$ allows the treatment intensity to vary throughout the domain, thereby representing geographical heterogeneity in healthcare accessibility, treatment coverage, or intervention effectiveness.

First, we illustrate the principal nonlocal components of the model in Figure 1. The left panel displays the Riesz fractional kernel associated with the regional fractional diffusion operator for $\alpha = 0.20$, whose singularity at the origin and algebraically decaying tail characterize the long-range dispersal permitted by fractional diffusion. The middle panel shows the Gaussian kernel employed in the nonlocal force of infection, where the interaction strength decreases smoothly with distance. The right panel presents the intermittent treatment protocol used throughout the numerical simulations, illustrating the periodic alternation between treatment and treatment-free intervals.

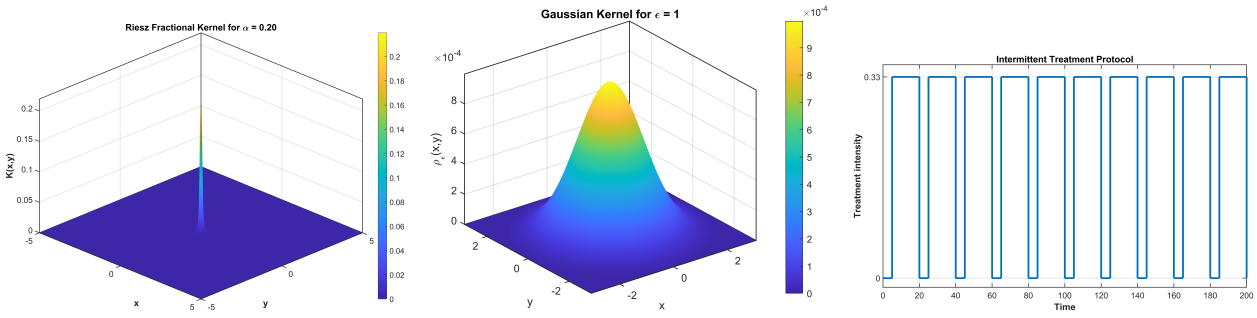


Figure 1: Fractional diffusion kernel, Gaussian transmission kernel, and intermittent treatment protocol.

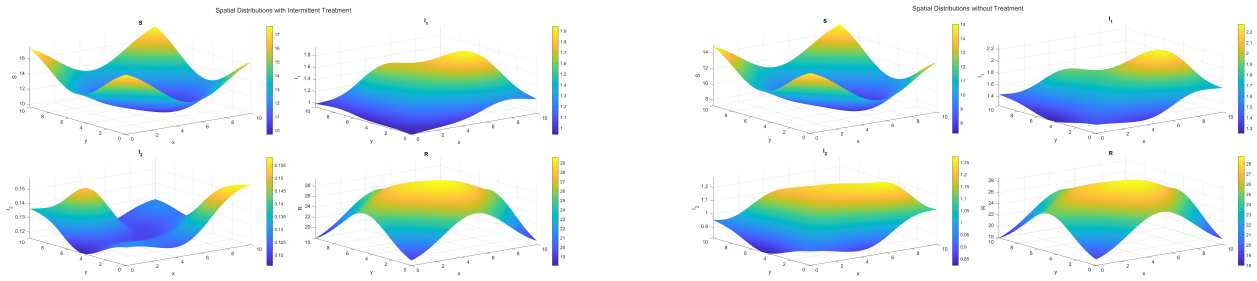


Figure 2: Spatial distributions of the susceptible (S), asymptomatic infected (I_1), symptomatic infected (I_2), and recovered (R) populations with and without intermittent treatment for $\alpha = 0.20$.

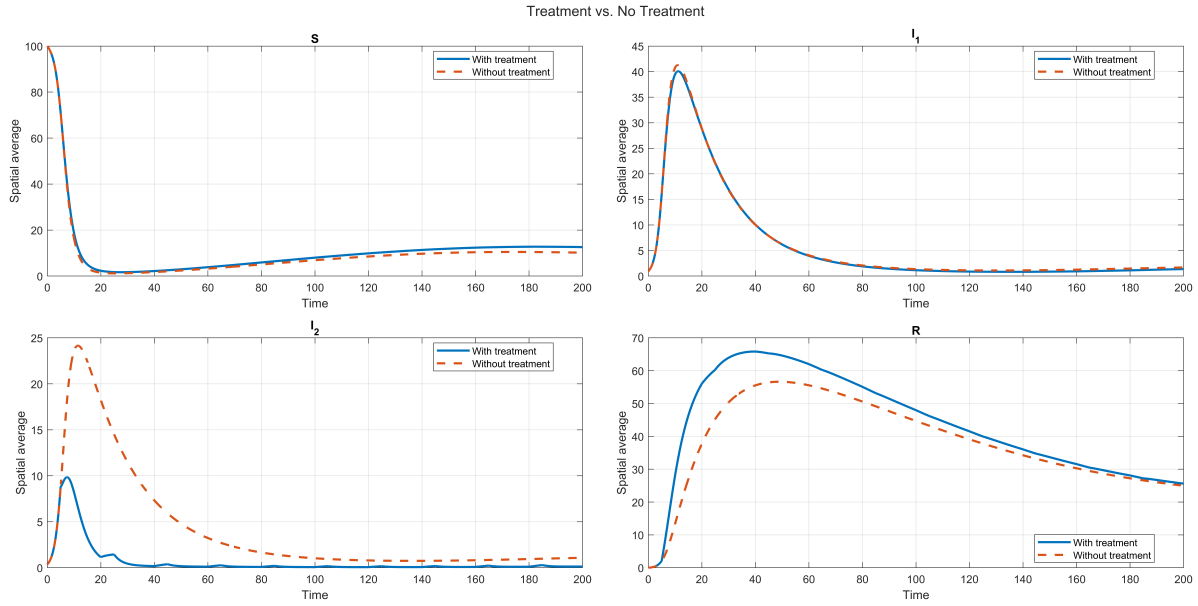


Figure 3: Spatial averages of the susceptible (S), asymptomatic infected (I_1), symptomatic infected (I_2), and recovered (R) populations with and without intermittent treatment for $\alpha = 0.20$.

Figure 2 presents the spatial distributions of the susceptible, asymptomatic infected, symptomatic infected, and recovered populations at the final simulation time for the fractional diffusion model with $\alpha = 0.20$. The heterogeneous spatial patterns arise from the combined effects of the regional fractional diffusion operator, the nonlocal Gaussian transmission kernel, and the spatially varying epidemiological coefficients. In both treatment scenarios, the compartment densities remain spatially nonuniform, reflecting

the underlying environmental heterogeneity. Comparing the two panels shows that intermittent treatment modifies the spatial distributions by increasing the susceptible population while reducing the densities of both asymptomatic and symptomatic infected individuals, accompanied by a corresponding change in the recovered population. These results demonstrate that the periodic treatment strategy influences not only the temporal dynamics but also the spatial organization of the epidemic.

The spatial distributions provide detailed information on the heterogeneous population dynamics. To obtain a global measure of these dynamics and to compare the treatment and no-treatment cases more clearly, we compute the spatial average of each population compartment,

$$\overline{U}(t) = \frac{1}{|\Omega|}\int_{\Omega} U(x,y,t)\,dx\,dy, \qquad U \in \{S, I_1, I_2, R\}. \tag{3.2}$$

Figure 3 presents the corresponding spatial averages of the four population compartments for the treatment and no-treatment scenarios. Consistent with the spatial distributions, intermittent treatment increases the average susceptible and recovered populations while substantially reducing the average symptomatic infected population. The effect on the asymptomatic infected population is comparatively moderate, indicating that the treatment primarily suppresses symptomatic infections and consequently mitigates disease transmission throughout the domain.

At last, to assess the role of crowding in disease transmission, we replace the reference crowding factor by two alternative crowding fields representing relatively small and large population densities, while keeping all remaining model parameters and initial conditions unchanged. Throughout this experiment, all model parameters, initial conditions, and the intermittent treatment strategy remain unchanged, while only the crowding factor is varied. Specifically, we consider the reference crowding field together with the following small- and large-crowd scenarios:

$$\omega_{\text{small}}(x,y) = 1.0 + 0.15\sin^2\!\left(\frac{\pi x}{L_x}\right)\sin^2\!\left(\frac{\pi y}{L_y}\right), \qquad \omega_{\text{large}}(x,y) = 3.00 + 1.00\sin^2\!\left(\frac{\pi x}{L_x}\right)\sin^2\!\left(\frac{\pi y}{L_y}\right).$$

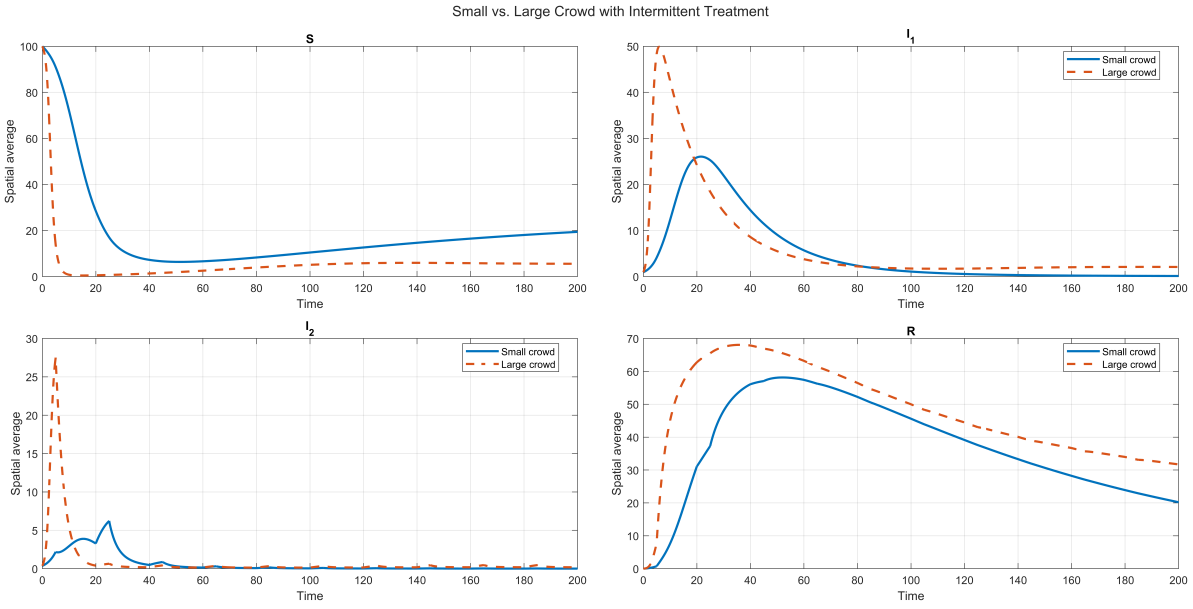


Figure 4: Spatial averages of the susceptible (S), asymptomatic infected (I_1), symptomatic infected (I_2), and recovered (R) populations under small- and large-crowd scenarios with intermittent treatment for $\alpha = 0.20$.

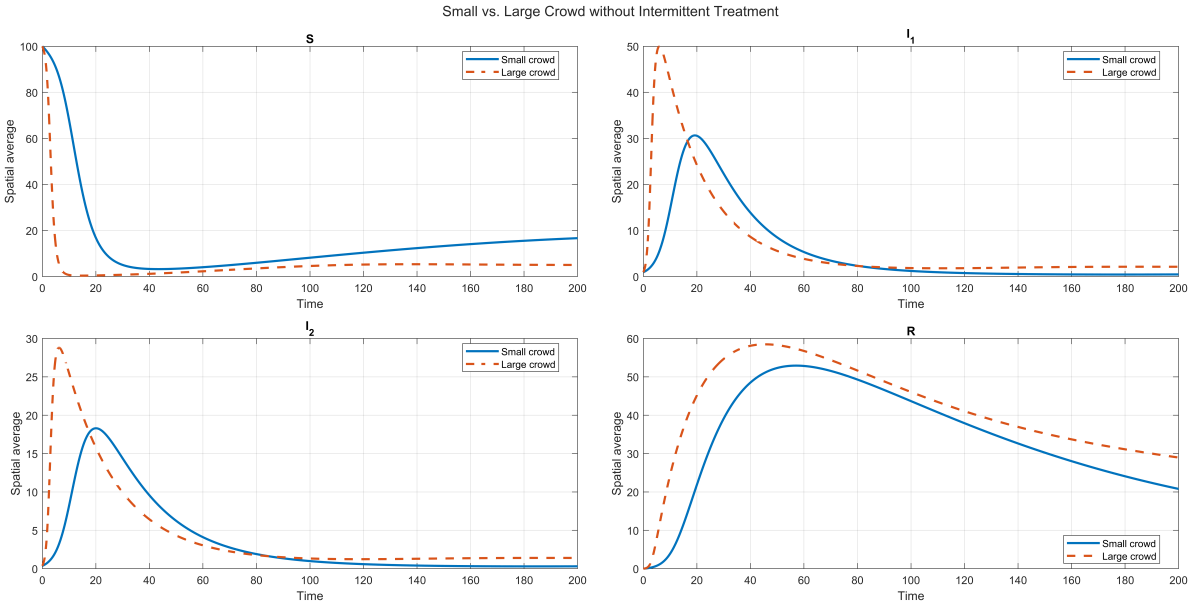


Figure 5: Spatial averages of the susceptible (S), asymptomatic infected (I_1), symptomatic infected (I_2), and recovered (R) populations under small- and large-crowd scenarios without intermittent treatment for $\alpha = 0.20$.

Figures 4 and 5 compare the spatial averages under small- and large-crowd scenarios in the absence and presence of intermittent treatment, respectively. In both cases, increasing the crowding factor accelerates disease transmission, leading to a more rapid depletion of the susceptible population and earlier, higher peaks in both the asymptomatic and symptomatic infected populations. Consequently, the recovered population increases more rapidly under the large-crowd scenario. In contrast, the small-crowd case exhibits slower epidemic progression, resulting in lower infection levels and a larger remaining susceptible population. The inclusion of intermittent treatment substantially suppresses the symptomatic infected population and increases the susceptible and recovered populations under both crowding scenarios. Nevertheless, the qualitative influence of crowding is preserved, demonstrating that higher crowd density consistently promotes disease transmission, whereas periodic treatment effectively mitigates its impact.

4 Conclusion

In this work, we investigated a spatiotemporal epidemic model incorporating regional fractional diffusion, nonlocal asymptomatic transmission, crowding-dependent disease transmission, and periodic intermittent treatment. By combining semigroup theory with L^p-energy estimates, we established the global existence, uniqueness, positivity, uniform boundedness, and asymptotic behavior of classical solutions. These analytical results provide a rigorous mathematical foundation for the proposed model and ensure the well-posedness of its long-term dynamics.

The numerical simulations complement the theoretical analysis by illustrating the spatiotemporal dynamics of the fractional diffusion model for different fractional diffusion exponents with nonlocal Gaussian transmission kernels, both in the presence and absence of intermittent treatment. In addition, the simulations investigate disease dynamics under relatively small and large crowding levels to assess the influence of population density on disease transmission. The numerical results demonstrate how regional fractional diffusion, nonlocal asymptomatic transmission, population crowding, heterogeneous epidemiological parameters, and periodic treatment jointly influence the temporal evolution and spatial distributions of the susceptible, asymptomatic infected, symptomatic infected, and recovered populations. They further show that variations in the fractional diffusion exponent, the spatial interaction range of the nonlocal transmission kernel, and the crowding level produce distinct qualitative patterns of disease spread and persistence.

The proposed framework provides a flexible mathematical setting for studying infectious disease transmission in heterogeneous environments where long-range mobility, asymptomatic transmission, and spatially varying intervention strategies play important roles. Future work may focus on incorporating more general regional fractional operators, alternative nonlocal transmission kernels, stochastic effects, data-driven parameter estimation, and optimal control strategies within fractional epidemic models.

Declaration of Interest Statement: The authors declare that they have no known competing financial interests or personal relationships that could have appeared to influence the work reported in this paper.

References

[1] Abdelmalek, S., and Kouachi, S. Proof of existence of global solutions for m-component reaction–diffusion systems with mixed boundary conditions via the lyapunov functional method. *Journal of Physics A: Mathematical and Theoretical 40*, 41 (2007), 12335–12350.

[2] Aguilar, J. B., and Gutierrez, J. B. An epidemiological model of malaria accounting for asymptomatic carriers. *Bulletin of mathematical biology 82*, 3 (2020), 42.

[3] Alam, M. S. Global analysis of the gray–scott model with fractional–classical diffusion. *Applicable Analysis* (2026), 1–16.

[4] Ammi, M. R. S., Zinihi, A., Raezah, A. A., and Sabbar, Y. Optimal control of a spatiotemporal sir model with reaction–diffusion involving p-laplacian operator. *Results in Physics 52* (2023), 106895.

[5] Andreu-Vaillo, F. *Nonlocal diffusion problems*. No. 165. American Mathematical Soc., 2010.

[6] Angstmann, C., Henry, B., and McGann, A. A fractional-order infectivity sir model. *Physica A: Statistical Mechanics and its Applications 452* (2016), 86–93.

[7] Angstmann, C. N., Henry, B. I., and McGann, A. V. A fractional-order infectivity and recovery sir model. *Fractal and Fractional 1*, 1 (2017), 11.

[8] Arendt, W. Vector-valued laplace transforms and cauchy problems. *Israel Journal of Mathematics 59*, 3 (1987), 327–352.

[9] Bai, F. An age-of-infection model with both symptomatic and asymptomatic infections. *Journal of Mathematical Biology 86*, 5 (2023), 82.

[10] Balzotti, C., D'Ovidio, M., and Loreti, P. Fractional sis epidemic models. *Fractal and Fractional 4*, 3 (2020), 44.

[11] Billingham, J. Dynamics of a strongly nonlocal reaction–diffusion population model. *Nonlinearity 17*, 1 (2004), 313–346.

[12] Colombo, R. M., and Garavello, M. Well posedness and control in a nonlocal sir model. *Applied Mathematics & Optimization 84*, 1 (2021), 737–771.

[13] Daoud, M., Laamri, E.-H., and Baalal, A. A class of fractional parabolic reaction–diffusion systems with control of total mass: theory and numerics. *Journal of Pseudo-Differential Operators and Applications 15*, 1 (2024), 18.

[14] Dey, S., and Kar, T. K. Dynamics of a nonlocal diffusive sir epidemic model with nonlocal infection. *Communications in Nonlinear Science and Numerical Simulation* (2025), 109161.

[15] Dipierro, S., Ros-Oton, X., and Valdinoci, E. Nonlocal problems with neumann boundary conditions. *Revista Matemática Iberoamericana 33*, 2 (2017), 377–416.

[16] Djenina, N., Ouannas, A., Batiha, I. M., Grassi, G., Oussaeif, T.-E., and Momani, S. A novel fractional-order discrete sir model for predicting covid-19 behavior. *Mathematics 10*, 13 (2022), 2224.

[17] Djilali, S., Chen, Y., and Bentout, S. Asymptotic analysis of sir epidemic model with nonlocal diffusion and generalized nonlinear incidence functional. *Mathematical Methods in the Applied Sciences 46*, 5 (2023), 6279–6301.

[18] Du, Q., GunzburGer, M., Lehoucq, R. B., and Zhou, K. A nonlocal vector calculus, nonlocal volume-constrained problems, and nonlocal balance laws. *Mathematical Models and Methods in Applied Sciences 23*, 03 (2013), 493–540.

[19] Fife, P. Some nonclassical trends in parabolic and parabolic-like evolutions. *Trends in nonlinear analysis* (2003), 153–191.

[20] Fitzgibbon, W., and Morgan, J. Analysis of a reaction diffusion model for a reservoir supported spread of infectious disease. *Discrete and Continuous Dynamical Systems-B 24*, 11 (2019), 6239–6259.

[21] Fitzgibbon, W., Morgan, J., Webb, G., and Wu, Y. Analysis of a reaction–diffusion epidemic model with asymptomatic transmission. *Journal of Biological Systems 28*, 03 (2020), 561–587.

[22] Goscé, L., Barton, D. A., and Johansson, A. Analytical modelling of the spread of disease in confined and crowded spaces. *Scientific reports 4*, 1 (2014), 4856.

[23] Guèrin, C., Girard, R., Selli, J., and Ayzac, L. Intermittent versus continuous renal replacement therapy for acute renal failure in intensive care units: results from a multicenter prospective epidemiological survey. *Intensive Care Medicine 28*, 10 (2002), 1411–1418.

[24] Guo, Z., Wang, F.-B., and Zou, X. Threshold dynamics of an infective disease model with a fixed latent period and non-local infections. *Journal of Mathematical Biology 65*, 6 (2012), 1387–1410.

[25] Guo, Z.-G., Sun, G.-Q., Wang, Z., Jin, Z., Li, L., and Li, C. Spatial dynamics of an epidemic model with nonlocal infection. *Applied Mathematics and Computation 377* (2020), 125158.

[26] Hamdan, N., and Kilicman, A. A fractional order sir epidemic model for dengue transmission. *Chaos, Solitons & Fractals 114* (2018), 55–62.

[27] Huo, J., and Zhao, H. Dynamical analysis of a fractional sir model with birth and death on heterogeneous complex networks. *Physica A: Statistical Mechanics and its Applications 448* (2016), 41–56.

[28] Kavallaris, N. I., and Suzuki, T. *Non-local partial differential equations for engineering and biology*. Springer, 2018.

[29] Kirschner, D., and Webb, G. F. A model for treatment strategy in the chemotherapy of aids. *Bulletin of mathematical biology 58*, 2 (1996), 367–390.

[30] Kouachi, S. Existence of global solutions to reaction-diffusion systems via a lyapunov functional. *Electronic Journal of Differential Equations (EJDE)[electronic only] 2001* (2001), Paper–No.

[31] Kuniya, T., and Wang, J. Global dynamics of an sir epidemic model with nonlocal diffusion. *Nonlinear Analysis: Real World Applications 43* (2018), 262–282.

[32] Laing, C. R., and Troy, W. C. Pde methods for nonlocal models. *SIAM Journal on Applied Dynamical Systems 2*, 3 (2003), 487–516.

[33] Leung, K. Y., Trapman, P., and Britton, T. Who is the infector? epidemic models with symptomatic and asymptomatic cases. *Mathematical biosciences 301* (2018), 190–198.

[34] Liu, Z., Shen, Z., Wang, H., and Jin, Z. Analysis of a local diffusive sir model with seasonality and nonlocal incidence of infection. *SIAM Journal on Applied Mathematics 79*, 6 (2019), 2218–2241.

[35] Lloyd, A. L., and May, R. M. Spatial heterogeneity in epidemic models. *Journal of theoretical biology 179*, 1 (1996), 1–11.

[36] Lunardi, A. *Analytic semigroups and optimal regularity in parabolic problems*. Springer Science & Business Media, 2012.

[37] Marques, J. C., Cezaro, A. D., and Lazo, M. J. A sir model with spatially distributed multiple populations interactions for disease dissemination. *Trends in Computational and Applied Mathematics 23*, 1 (2022), 143–154.

[38] McKendrick, A. The dynamics of crowd infection. *Edinburgh Medical Journal 47*, 2 (1940), 117.

[39] Milner, F. A., and Zhao, R. Sir model with directed spatial diffusion. *Mathematical Population Studies 15*, 3 (2008), 160–181.

[40] Nezza, E. D., Palatucci, G., and Valdinoci, E. Hitchhiker's guide to the fractional sobolev spaces. *Bulletin des sciences mathématiques 136*, 5 (2012), 521–573.

[41] Paeng, S.-H., and Lee, J. Continuous and discrete sir-models with spatial distributions. *Journal of mathematical biology 74*, 7 (2017), 1709–1727.

[42] Parkinson, C., and Wang, W. Analysis of a reaction-diffusion sir epidemic model with noncompliant behavior. *SIAM Journal on Applied Mathematics 83*, 5 (2023), 1969–2002.

[43] Pazy, A. *Semigroups of Linear Operators and Applications to Partial Differential Equations*, vol. 44 of *Applied Mathematical Sciences*. Springer, 2012.

[44] Ross, A., Penny, M., Maire, N., Studer, A., Carneiro, I., Schellenberg, D., Greenwood, B., Tanner, M., and Smith, T. Modelling the epidemiological impact of intermittent preventive treatment against malaria in infants. *PLoS One 3*, 7 (2008), e2661.

[45] Ruan, S. Spatial-temporal dynamics in nonlocal epidemiological models. In *Mathematics for life science and medicine*. Springer, 2007, pp. 97–122.

[46] Saad-Roy, C. M., Wingreen, N. S., Levin, S. A., and Grenfell, B. T. Dynamics in a simple evolutionary-epidemiological model for the evolution of an initial asymptomatic infection stage. *Proceedings of the national academy of sciences 117*, 21 (2020), 11541–11550.

[47] Taghvaei, A., Georgiou, T. T., Norton, L., and Tannenbaum, A. Fractional sir epidemiological models. *Scientific reports 10*, 1 (2020), 20882.

[48] Triebel, H. *Theory of function spaces III*. Springer, 2006.

[49] Wang, J.-B., Li, W.-T., and Yang, F.-Y. Traveling waves in a nonlocal dispersal sir model with nonlocal delayed transmission. *Communications in Nonlinear Science and Numerical Simulation 27*, 1-3 (2015), 136–152.

[50] Wang, W., and Zhao, X.-Q. A nonlocal and time-delayed reaction-diffusion model of dengue transmission. *SIAM Journal on Applied Mathematics 71*, 1 (2011), 147–168.

[51] Wang, W., and Zhao, X.-Q. Basic reproduction numbers for reaction-diffusion epidemic models. *SIAM Journal on Applied Dynamical Systems 11*, 4 (2012), 1652–1673.

[52] Yang, C., and Wang, J. Basic reproduction numbers for a class of reaction-diffusion epidemic models. *Bulletin of mathematical biology 82* (2020), 1–25.

[53] Yang, F.-Y., Li, Y., Li, W.-T., and Wang, Z.-C. Traveling waves in a nonlocal dispersal kermack-mckendrick epidemic model. *Discrete & Continuous Dynamical Systems-Series B 18*, 7 (2013).

[54] Yang, S., Chu, W., and Kevrekidis, P. An epidemical model with nonlocal spatial infections. *Proceedings of the European Academy of Sciences and Arts 3*, 1 (2025).

[55] Zhang, G.-B., Li, W.-T., and Wang, Z.-C. Spreading speeds and traveling waves for nonlocal dispersal equations with degenerate monostable nonlinearity. *Journal of Differential Equations 252*, 9 (2012), 5096–5124.

[56] Zhao, G., and Ruan, S. Spatial and temporal dynamics of a nonlocal viral infection model. *SIAM Journal on Applied Mathematics 78*, 4 (2018), 1954–1980.

[57] Zhao, M., Li, W., and Cao, J. Dynamics for an sir epidemic model with nonlocal diffusion and free boundaries. *Acta Mathematica Scientia 41*, 4 (2021), 1081–1106.

[58] Zhao, X.-D., Li, W.-T., and Bao, X. Spatial dynamics of a nonlocal dispersal sir epidemic model with recruitment in time heterogeneous media. *Journal of Dynamics and Differential Equations* (2025), 1–36.

[59] Zhou, J., Dong, S., Ma, C., Wu, Y., and Qiu, X. Epidemic spread simulation in an area with a high-density crowd using a seir-based model. *PLoS One 16*, 6 (2021), e0253220.